RESEARCH ARTICLE | OCTOBER 22 2024

Calculation of tearing mode stability in an inverse aspect-ratio expanded tokamak plasma equilibrium

Richard Fitzpatrick

Phys. Plasmas 31, 102507 (2024)
https://doi.org/10.1063/5.0231715

Physics of Plasmas ARTICLE pubs.aip.org/aip/pop

Calculation of tearing mode stability in an inverse aspect-ratio expanded tokamak plasma equilibrium

Cite as: Phys. Plasmas **31**, 102507 (2024); doi: 10.1063/5.0231715
Submitted: 1 August 2024 · Accepted: 4 October 2024 ·
Published Online: 22 October 2024

Richard Fitzpatrick[a)]

AFFILIATIONS

Institute for Fusion Studies, Department of Physics, University of Texas at Austin, Austin, Texas 78712, USA

[a)]Author to whom correspondence should be addressed: rfitzp@utexas.edu

ABSTRACT

The tearing mode stability of an inverse aspect-ratio expanded tokamak plasma equilibrium of general shape is investigated using asymptotic matching techniques. Particular emphasis is placed on the conservation of toroidal electromagnetic angular momentum. The TJ code, which is a specific implementation of the results of the investigation, is described.

I. INTRODUCTION

The calculation of the tearing mode stability of a high temperature, axisymmetric, tokamak plasma equilibrium is most efficiently formulated as an asymptotic matching problem.[1] In such a problem, the plasma is divided into two regions. In the "outer region," which comprises most of the plasma, the tearing perturbation is described by the equations of linearized, marginally stable, ideal magnetohydrodynamics (which, in the following, are referred to as the "ideal-MHD" equations) (see Sec. III B). However, these equations become singular on so-called "rational" magnetic flux surfaces at which the perturbed magnetic field resonates with the equilibrium field. In the so-called "inner region," which consists of a set of narrow layers centered on the various rational surfaces, non-ideal-MHD effects such as plasma inertia, resistivity, and viscosity become important. The growth rate and angular rotation frequency of the reconnected magnetic flux at a given rational surface (numbered k) are fixed by asymptotically matching the resistive layer solution in the associated segment of the inner region, which is characterized by a dimensionless complex quantity Δ_k, to the ideal-MHD solution in the outer region. In a realistic axisymmetric tokamak plasma equilibrium, tearing perturbations with different toroidal mode numbers are independent of one another, whereas perturbations with different poloidal mode numbers are coupled together via toroidicity and the non-circular shaping of equilibrium magnetic flux surfaces.[2] Consequently, for a tearing perturbation with a given toroidal mode number, the Δ_k values associated with the various rational surfaces in the plasma are interrelated via a matrix equation[3] [see Eq. (319)].

In general, the determination of the elements of the matrix equation that links the various Δ_k values from the ideal-MHD equations in the outer region is an exceptionally challenging computational task.[4–19] One way of greatly reducing the complexity of this task is to employ an inverse aspect-ratio expanded plasma equilibrium.[20,21] In such an equilibrium, the metric elements of the flux-coordinate system can be expressed analytically in terms of a relatively small number of flux-surface functions, which represents a major simplification.[2] Another significant advantage of an inverse aspect-ratio expanded equilibrium is that the magnetic perturbation in the plasma can be efficiently matched to an exterior vacuum solution that is expressed as an expansion in toroidal functions.[6] The alternative approach of using a Green's function solution in the vacuum region is much more computationally intensive.[22,23]

The inverse aspect-ratio expansion approach to determining tearing mode stability in tokamak plasmas was first presented in Ref. 4, in a calculation that features triplets of poloidal harmonics coupled via toroidicity. The inverse aspect-ratio expansion approach was extended in Ref. 6, in a calculation that features septuplets of poloidal harmonics coupled via toroidicity, flux-surface elongation, and flux-surface triangularity. In this paper, we generalize the inverse aspect-ratio expansion approach to allow for an *arbitrary* number of poloidal harmonics coupled by flux surfaces of *general* shape. Furthermore, unlike Refs. 4 and 6, we do not assume that the plasma equilibrium is up-down-symmetric.

This paper is organized as follows. In Sec. II, we examine a general tokamak plasma equilibrium. In Sec. III, we derive the so-called

"outer-region partial differential equations (p.d.e.s)," which are a set of two coupled second-order p.d.e.s that control the ideal-MHD solution in the outer region. In Sec. IV, we derive the so-called "outer-region ordinary differential equations (o.d.e.s)," which are a large set of coupled first-order o.d.e.s that control the ideal-MHD solution in the outer region. We also demonstrate that these o.d.e.s conserve toroidal electromagnetic angular momentum. In Sec. V, we discuss the general behavior of the outer-region o.d.e.s in the vicinity of a rational surface. In Sec. VI, we obtain the general boundary condition satisfied by the outer-region o.d.e.s at the plasma/vacuum interface, on the assumption that the region surrounding the plasma does not contain any non-axisymmetric currents. We also demonstrate that these boundary conditions conserve toroidal electromagnetic angular momentum. In Sec. VII, we introduce the aspect-ratio expanded tokamak equilibrium and determine the specific forms of the outer-region o.d.e.s. In Sec. VIII, we calculate the matrix equation that constitutes the tearing mode dispersion relation and demonstrate that this equation must be Hermitian in order to conserve toroidal electromagnetic angular momentum. In Sec. IX, we discuss how the tearing mode dispersion relation is modified by non-axisymmetric currents flowing in resonant magnetic perturbation (RMP) coils external to the plasma. We also derive expressions for the toroidal electromagnetic torques exerted at the various rational surfaces in the plasma by the RMP coils. In Sec. X, we discuss the TJ code, which is a specific implementation of the theory presented in Sec. II–IX. Finally, the paper is summarized in Sec. XI.

II. GENERAL PLASMA EQUILIBRIUM

A. Normalization

All lengths in this paper are normalized to the major radius of the plasma magnetic axis, R_0. All magnetic field strengths are normalized to the toroidal field strength at the magnetic axis, B_0. All currents are normalized to $B_0\,R_0/\mu_0$. All current densities are normalized to $B_0/(\mu_0\,R_0)$. All plasma pressures are normalized to B_0^2/μ_0. All toroidal electromagnetic torques are normalized to $B_0^2\,R_0^3/\mu_0$.

B. Axisymmetric tokamak plasma equilibrium

Let R, ϕ, and Z be right-handed cylindrical coordinates whose Jacobian is

$$(\nabla R\times\nabla\phi\cdot\nabla Z)^{-1}=R. \tag{1}$$

Note that $|\nabla\phi|=1/R$.

Let r, θ, and ϕ be right-handed flux-coordinates whose Jacobian is[4,24]

$$\mathcal{J}(r,\theta)\equiv(\nabla r\times\nabla\theta\cdot\nabla\phi)^{-1}\equiv R\left(\frac{\partial R}{\partial\theta}\frac{\partial Z}{\partial r}-\frac{\partial R}{\partial r}\frac{\partial Z}{\partial\theta}\right)=r\,R^2. \tag{2}$$

Note that $r=r(R,Z)$ and $\theta=\theta(R,Z)$. The magnetic axis corresponds to $r=0$. The inboard mid-plane corresponds to $\theta=0$.

Consider an axisymmetric tokamak equilibrium[25] whose magnetic field takes the form[4,6]

$$\mathbf{B}(r,\theta)=f(r)\,\nabla\phi\times\nabla r+g(r)\,\nabla\phi=f\,\nabla(\phi-q\,\theta)\times\nabla r, \tag{3}$$

where

$$q(r)=\frac{r\,g}{f} \tag{4}$$

is the safety factor (i.e., the inverse of the rotational transform). Note that $\mathbf{B}\cdot\nabla r=0$, which implies that r is a magnetic flux-surface label. We require $g=1$ on the magnetic axis in order to ensure that the normalized toroidal magnetic field-strength at the axis is unity.

It is easily demonstrated that

$$B^r=\mathbf{B}\cdot\nabla r=0, \tag{5}$$

$$B^\theta=\mathbf{B}\cdot\nabla\theta=\frac{f}{r\,R^2}, \tag{6}$$

$$B^\phi=\mathbf{B}\cdot\nabla\phi=\frac{g}{R^2}, \tag{7}$$

$$B_r=\mathcal{J}\,\nabla\theta\times\nabla\phi\cdot\mathbf{B}=-r f\,\nabla r\cdot\nabla\theta, \tag{8}$$

$$B_\theta=\mathcal{J}\,\nabla\phi\times\nabla r\cdot\mathbf{B}=r f\,|\nabla r|^2, \tag{9}$$

$$B_\phi=\mathcal{J}\,\nabla r\times\nabla\theta\cdot\mathbf{B}=g, \tag{10}$$

where use has been made of the results and notation of the Appendix.

The Maxwell equation (neglecting the displacement current, because tearing modes are comparatively low-frequency phenomena) $\mathbf{J}=\nabla\times\mathbf{B}$ yields

$$\mathcal{J}\,J^r=\frac{\partial B_\phi}{\partial\theta}=0, \tag{11}$$

$$\mathcal{J}\,J^\theta=-\frac{\partial B_\phi}{\partial r}=-g', \tag{12}$$

$$\mathcal{J}\,J^\phi=\frac{\partial B_\theta}{\partial r}-\frac{\partial B_r}{\partial\theta}=\frac{\partial}{\partial r}\left(r f\,|\nabla r|^2\right)+\frac{\partial}{\partial\theta}\left(r f\,\nabla r\cdot\nabla\theta\right), \tag{13}$$

where $\mathbf{J}$ is the equilibrium current density, $'\equiv d/dr$, and use has been made of Eqs. (8)–(10) and (A11)–(A13).

Equilibrium force balance requires that

$$\nabla P=\mathbf{J}\times\mathbf{B}, \tag{14}$$

where $P(r)$ is the equilibrium scalar plasma pressure. Here, for the sake of simplicity, we have neglected the small centrifugal modifications to force balance due to subsonic plasma rotation.[26,27] It follows that

$$\begin{aligned}P'&=\mathcal{J}(J^\theta\,B^\phi-J^\phi\,B^\theta)\\&=-g'\,\frac{g}{R^2}-\frac{f}{r\,R^2}\left[\frac{\partial}{\partial r}\left(r f\,|\nabla r|^2\right)+\frac{\partial}{\partial\theta}\left(r f\,\nabla r\cdot\nabla\theta\right)\right],\end{aligned} \tag{15}$$

where use has been made of Eqs. (5)–(7), (11)–(13), and (A4)–(A6). The other two components of Eq. (14) are identically zero.

Equation (15) yields the *Grad–Shafranov equation*,[25]

$$\frac{f}{r}\frac{\partial}{\partial r}\left(r f\,|\nabla r|^2\right)+\frac{f}{r}\frac{\partial}{\partial\theta}\left(r f\,\nabla r\cdot\nabla\theta\right)+g\,g'+R^2\,P'=0. \tag{16}$$

It follows from Eqs. (4), (13), and (16) that

$$\mathcal{J}\,J^\phi=-q\,g'-\frac{r\,R^2\,P'}{f}. \tag{17}$$

It is clear from Eqs. (12) and (17) that $g'=P'=0$ in the current-free "vacuum" region surrounding the plasma. We shall also assume that $g'=P'=0$ at the plasma/vacuum interface, so as to ensure that the equilibrium plasma current density is zero at the interface.

III. DERIVATION OF OUTER-REGION P.D.E.S

A. Introduction

The outer-region p.d.e.s were first presented in Ref. 4, without an explicit derivation. However, the derivation is sufficiently non-obvious that it is worth outlining in this section.

B. Governing equations

In the outer region, the perturbed plasma equilibrium satisfies the ideal-MHD equations[4,6,16,25]

$$\mathbf{b} = \nabla \times (\boldsymbol{\xi} \times \mathbf{B}), \tag{18}$$

$$\nabla p = \mathbf{j} \times \mathbf{B} + \mathbf{J} \times \mathbf{b}, \tag{19}$$

$$\mathbf{j} = \nabla \times \mathbf{b}, \tag{20}$$

$$p = -\boldsymbol{\xi} \cdot \nabla P, \tag{21}$$

where $\boldsymbol{\xi}(r,\theta,\phi)$ is the plasma displacement, $\mathbf{b}(r,\theta,\phi)$ the perturbed magnetic field, $\mathbf{j}(r,\theta,\phi)$ the perturbed current density, and $p(r,\theta,\phi)$ the perturbed scalar pressure. Let us assume that all perturbed quantities vary with the toroidal angle, ϕ, as $\exp(-\mathrm{i}\, n\, \phi)$, where the real positive integer n is the toroidal mode number of the tearing mode. For example, $p(r,\theta,\phi) = p(r,\theta)\, \exp(-\mathrm{i}\, n\, \phi)$.

C. Radial plasma displacement

Equations (A5) and (A6) yield

$$(\boldsymbol{\xi} \times \mathbf{B})_\theta = \mathcal{J}\, (\xi^\phi\, B^r - \xi^r\, B^\phi) = -\mathcal{J}\, B^\phi\, \xi^r, \tag{22}$$

$$(\boldsymbol{\xi} \times \mathbf{B})_\phi = \mathcal{J}\, (\xi^r\, B^\theta - \xi^\theta\, B^r) = \mathcal{J}\, B^\theta\, \xi^r, \tag{23}$$

where use has been made of the fact that $B^r = J^r = 0$ [see Eqs. (5) and (11)]. Combining the previous two equations with Eqs. (18) and (A11), we obtain

$$\mathcal{J}\, b^r = \frac{\partial}{\partial \theta}\left(\mathcal{J}\, B^\theta\, \xi^r\right) - \mathrm{i}\, n\, \mathcal{J}\, B^\phi\, \xi^r. \tag{24}$$

Thus, Eqs. (2), (4), (6), and (7) give

$$r\, R^2\, b^r = \left(\frac{\partial}{\partial \theta} - \mathrm{i}\, n\, q\right) y, \tag{25}$$

where

$$y(r,\theta) = f\, \xi^r. \tag{26}$$

D. Perturbed force balance

According to Eq. (21),

$$p = -P'\, \nabla r \cdot \boldsymbol{\xi} = -P'\, \xi^r. \tag{27}$$

So, the perturbed force balance equation (19) yields

$$-\frac{\partial\, (P'\, \xi^r)}{\partial r} = (\mathbf{j} \times \mathbf{B})_r + (\mathbf{J} \times \mathbf{b})_r, \tag{28}$$

$$-\frac{\partial\, (P'\, \xi^r)}{\partial \theta} = (\mathbf{j} \times \mathbf{B})_\theta + (\mathbf{J} \times \mathbf{b})_\theta, \tag{29}$$

$$\mathrm{i}\, n\, P'\, \xi^r = (\mathbf{j} \times \mathbf{B})_\phi + (\mathbf{J} \times \mathbf{b})_\phi, \tag{30}$$

giving

$$-\frac{\partial\, (P'\, \xi^r)}{\partial r} = r\, R^2\, (j^\theta\, B^\phi - j^\phi\, B^\theta) + r\, R^2\, (J^\theta\, b^\phi - J^\phi\, b^\theta), \tag{31}$$

$$-\frac{\partial\, (P'\, \xi^r)}{\partial \theta} = r\, R^2\, (j^\phi\, B^r - j^r\, B^\phi) + r\, R^2\, (J^\phi\, b^r - J^r\, b^\phi), \tag{32}$$

$$\mathrm{i}\, n\, P'\, \xi^r = r\, R^2\, (j^r\, B^\theta - j^\theta\, B^r) + r\, R^2\, (J^r\, b^\theta - J^\theta\, b^r), \tag{33}$$

where use has been made of Eqs. (2) and (A4)–(A6). Thus, according to Eqs. (5)–(7), (11), (12), and (17),

$$-\frac{\partial\, (P'\, \xi^r)}{\partial r} = f\, (q\, j^\theta - j^\phi) - g'\, b^\phi + \left(q\, g' + \frac{r\, R^2\, P'}{f}\right) b^\theta, \tag{34}$$

$$-\frac{\partial\, (P'\, \xi^r)}{\partial \theta} = -r\, g\, j^r - \left(q\, g' + \frac{r\, R^2\, P'}{f}\right) b^r, \tag{35}$$

$$\mathrm{i}\, n\, P'\, \xi^r = f\, j^r + g'\, b^r. \tag{36}$$

It follows from Eqs. (26), (25), and (36) that

$$r\, j^r = \mathrm{i}\, n\, \alpha_p\, y - \frac{\alpha_g}{R^2}\left(\frac{\partial}{\partial \theta} - \mathrm{i}\, n\, q\right) y, \tag{37}$$

where

$$\alpha_p(r) = \frac{r\, P'}{f^2}, \tag{38}$$

$$\alpha_g(r) = \frac{g'}{f}. \tag{39}$$

Note that Eq. (35) is trivially satisfied. Hence, of the three components of the perturbed force balance equation, only Eq. (34) remains to be solved.

E. Perturbed plasma current density

Equation (20) yields

$$r\, R^2\, j^r = \frac{\partial b_\phi}{\partial \theta} + \mathrm{i}\, n\, b_\theta, \tag{40}$$

$$r\, R^2\, j^\theta = -\mathrm{i}\, n\, b_r - \frac{\partial b_\phi}{\partial r}, \tag{41}$$

$$r\, R^2\, j^\phi = \frac{\partial b_\theta}{\partial r} - \frac{\partial b_r}{\partial \theta}, \tag{42}$$

where use has been made of Eqs. (2) and (A11)–(A13).

F. Perturbed magnetic field

According to the Appendix,

$$\mathbf{b} = b_r\, \nabla r + b_\theta\, \nabla \theta + b_\phi\, \nabla \phi, \tag{43}$$

so

$$b^r = \mathbf{b} \cdot \nabla r = |\nabla r|^2\, b_r + (\nabla r \cdot \nabla \theta)\, b_\theta, \tag{44}$$

$$b^\theta = \mathbf{b} \cdot \nabla \theta = (\nabla r \cdot \nabla \theta)\, b_r + |\nabla \theta|^2\, b_\theta, \tag{45}$$

$$b^\phi = \mathbf{b} \cdot \nabla \phi = \frac{b_\phi}{R^2}. \tag{46}$$

Let us define

$$x(r,\theta) = b_\phi. \tag{47}$$

It follows from Eqs. (37), (40), (46), and (47) that

$$b_\theta = -\frac{\alpha_g}{\mathrm{i}\,n}\left(\frac{\partial}{\partial\theta} - \mathrm{i}\,n\,q\right)y + \alpha_p\,R^2\,y - \frac{1}{\mathrm{i}\,n}\frac{\partial x}{\partial\theta}, \tag{48}$$

$$b^\phi = \frac{x}{R^2}. \tag{49}$$

Equations (44) and (45) can be rearranged to give

$$b_r = \left(\frac{1}{|\nabla r|^2}\right)b^r - \left(\frac{\nabla r\cdot\nabla\theta}{|\nabla r|^2}\right)b_\theta, \tag{50}$$

$$b^\theta = \left(\frac{\nabla r\cdot\nabla\theta}{|\nabla r|^2}\right)b^r + \left[|\nabla\theta|^2 - \frac{(\nabla r\cdot\nabla\theta)^2}{|\nabla r|^2}\right]b_\theta. \tag{51}$$

However, from Eq. (2),

$$|\nabla r|^2\,|\nabla\theta|^2 - (\nabla r\cdot\nabla\theta)^2 = \frac{1}{r^2\,R^2}. \tag{52}$$

Thus, Eq. (51) reduces to

$$b^\theta = \left(\frac{\nabla r\cdot\nabla\theta}{|\nabla r|^2}\right)b^r + \left(\frac{1}{r^2\,R^2\,|\nabla r|^2}\right)b_\theta. \tag{53}$$

Making use of Eqs. (25) and (48), we obtain

$$r^2\,R^2\,b^\theta = T\left(\frac{\partial}{\partial\theta} - \mathrm{i}\,n\,q\right)y + U\,y - Q\,\frac{\partial x}{\partial\theta}, \tag{54}$$

where

$$Q(r,\theta) = \frac{1}{\mathrm{i}\,n\,|\nabla r|^2}, \tag{55}$$

$$U(r,\theta) = \frac{\alpha_p\,R^2}{|\nabla r|^2}, \tag{56}$$

$$T(r,\theta) = \frac{r\,\nabla r\cdot\nabla\theta}{|\nabla r|^2} - \frac{\alpha_g}{\mathrm{i}\,n\,|\nabla r|^2}. \tag{57}$$

Equation (50) gives

$$b_r = A\left(\frac{\partial}{\partial\theta} - \mathrm{i}\,n\,q\right)y - B\,y + C\,\frac{\partial x}{\partial\theta}, \tag{58}$$

where

$$A(r,\theta) = \frac{1}{r\,R^2\,|\nabla r|^2} + \frac{\alpha_g}{\mathrm{i}\,n}\,\frac{\nabla r\cdot\nabla\theta}{|\nabla r|^2}, \tag{59}$$

$$B(r,\theta) = \alpha_p\,\frac{R^2\,\nabla r\cdot\nabla\theta}{|\nabla r|^2}, \tag{60}$$

$$C(r,\theta) = \frac{1}{\mathrm{i}\,n}\,\frac{\nabla r\cdot\nabla\theta}{|\nabla r|^2}, \tag{61}$$

and use has been made of Eqs. (25) and (48).

G. First outer-region P.D.E.

According to Eq. (18),

$$\nabla\cdot\mathbf{b} = 0, \tag{62}$$

which implies that

$$r\,\frac{\partial}{\partial r}\left[\left(\frac{\partial}{\partial\theta} - \mathrm{i}\,n\,q\right)y\right] + \frac{\partial(r^2\,R^2\,b^\theta)}{\partial\theta} - S\,x = 0, \tag{63}$$

where

$$S(r) = \mathrm{i}\,n\,r^2, \tag{64}$$

and use has been made of Eqs. (2), (25), (49), and (A10). Thus, employing Eq. (54), we obtain the *first outer-region p.d.e.*,[4]

$$r\,\frac{\partial}{\partial r}\left[\left(\frac{\partial}{\partial\theta} - \mathrm{i}\,n\,q\right)y\right] = \frac{\partial}{\partial\theta}\left(Q\,\frac{\partial x}{\partial\theta}\right) + S\,x - \frac{\partial}{\partial\theta}\left[T\left(\frac{\partial}{\partial\theta} - \mathrm{i}\,n\,q\right)y + U\,y\right]. \tag{65}$$

H. Second outer-region P.D.E.

According to Eqs. (41), (42), (47), (48), and (58),

$$r\,R^2\,j^\theta = -\mathrm{i}\,n\left[A\left(\frac{\partial}{\partial\theta} - \mathrm{i}\,n\,q\right)y - B\,y + C\,\frac{\partial x}{\partial\theta}\right] - \frac{\partial x}{\partial r}, \tag{66}$$

$$r\,R^2\,j^\phi = \frac{\partial}{\partial r}\left[-\frac{\alpha_g}{\mathrm{i}\,n}\left(\frac{\partial}{\partial\theta} - \mathrm{i}\,n\,q\right)y + \alpha_p\,R^2\,y\right] - \frac{1}{\mathrm{i}\,n}\,\frac{\partial^2 x}{\partial r\,\partial\theta} - \frac{\partial}{\partial\theta}\left[A\left(\frac{\partial}{\partial\theta} - \mathrm{i}\,n\,q\right)y - B\,y + C\,\frac{\partial x}{\partial\theta}\right]. \tag{67}$$

So,

$$r\,R^2\,(q\,j^\theta - j^\phi) = \left(\frac{\partial}{\partial\theta} - \mathrm{i}\,n\,q\right)\left[A\left(\frac{\partial}{\partial\theta} - \mathrm{i}\,n\,q\right)y - B\,y + C\,\frac{\partial x}{\partial\theta}\right] + \frac{1}{\mathrm{i}\,n}\left(\frac{\partial}{\partial\theta} - \mathrm{i}\,n\,q\right)\frac{\partial x}{\partial r} - \frac{\partial}{\partial r}\left[-\frac{\alpha_g}{\mathrm{i}\,n}\left(\frac{\partial}{\partial\theta} - \mathrm{i}\,n\,q\right)y + \alpha_p\,R^2\,y\right]. \tag{68}$$

Thus, Eq. (34) gives

$$-\frac{r\,R^2}{f}\,\frac{\partial}{\partial r}\left(\frac{f}{r}\,\alpha_p\,y\right) = \left(\frac{\partial}{\partial\theta} - \mathrm{i}\,n\,q\right)\left[A\left(\frac{\partial}{\partial\theta} - \mathrm{i}\,n\,q\right)y - B\,y + C\,\frac{\partial x}{\partial\theta}\right] + \frac{1}{\mathrm{i}\,n}\left(\frac{\partial}{\partial\theta} - \mathrm{i}\,n\,q\right)\frac{\partial x}{\partial r} - \frac{\partial}{\partial r}\left[-\frac{\alpha_g}{\mathrm{i}\,n}\left(\frac{\partial}{\partial\theta} - \mathrm{i}\,n\,q\right)y + \alpha_p\,R^2\,y\right] - r\,\alpha_g\,x + \frac{1}{r}\,(q\,\alpha_g + R^2\,\alpha_p)\left[T\left(\frac{\partial}{\partial\theta} - \mathrm{i}\,n\,q\right)y + U\,y - Q\,\frac{\partial x}{\partial\theta}\right], \tag{69}$$

where use has been made of Eqs. (26), (38), (39), (49), and (54). The previous equation reduces to

$$-\mathrm{i}n\alpha_p\alpha_f R^2 y = \mathrm{i}n\left(\frac{\partial}{\partial\theta}-\mathrm{i}nq\right)\left[rA\left(\frac{\partial}{\partial\theta}-\mathrm{i}nq\right)y - rBy + rC\frac{\partial x}{\partial\theta}\right] + \left(\frac{\partial}{\partial\theta}-\mathrm{i}nq\right)r\frac{\partial x}{\partial r} + r\alpha_g'\left(\frac{\partial}{\partial\theta}-\mathrm{i}nq\right)y + \alpha_g r\frac{\partial}{\partial r}\left[\left(\frac{\partial}{\partial\theta}-\mathrm{i}nq\right)y\right] - \mathrm{i}nr\frac{\partial R^2}{\partial r}\alpha_p y - \alpha_g S x + \mathrm{i}n\left(q\alpha_g + R^2\alpha_p\right)\left[T\left(\frac{\partial}{\partial\theta}-\mathrm{i}nq\right)y + Uy - Q\frac{\partial x}{\partial\theta}\right], \tag{70}$$

where

$$\alpha_f(r) = \frac{r^2}{f}\frac{d}{dr}\left(\frac{f}{r}\right), \tag{71}$$

and use has been made of Eq. (64). Employing Eq. (65), we obtain

$$\begin{aligned}-\mathrm{i}n\alpha_p\alpha_f R^2 y &= \mathrm{i}n\left(\frac{\partial}{\partial\theta}-\mathrm{i}nq\right)\left[rA\left(\frac{\partial}{\partial\theta}-\mathrm{i}nq\right)y - rBy + rC\frac{\partial x}{\partial\theta}\right] + \left(\frac{\partial}{\partial\theta}-\mathrm{i}nq\right)r\frac{\partial x}{\partial r} + r\alpha_g'\left(\frac{\partial}{\partial\theta}-\mathrm{i}nq\right)y \\ &+ \alpha_g\frac{\partial}{\partial\theta}\left(Q\frac{\partial x}{\partial\theta}\right) + \alpha_g S x - \alpha_g\frac{\partial}{\partial\theta}\left[T\left(\frac{\partial}{\partial\theta}-\mathrm{i}nq\right)y + Uy\right] \\ &- \mathrm{i}nr\frac{\partial R^2}{\partial r}\alpha_p y - \alpha_g S x + \mathrm{i}n\left(q\alpha_g + R^2\alpha_p\right) \\ &\times\left[T\left(\frac{\partial}{\partial\theta}-\mathrm{i}nq\right)y + Uy - Q\frac{\partial x}{\partial\theta}\right],\end{aligned} \tag{72}$$

which yields

$$\begin{aligned}-\mathrm{i}n\alpha_p\alpha_f R^2 y &= \mathrm{i}n\left(\frac{\partial}{\partial\theta}-\mathrm{i}nq\right)\left[rA\left(\frac{\partial}{\partial\theta}-\mathrm{i}nq\right)y - rBy + rC\frac{\partial x}{\partial\theta}\right] + \left(\frac{\partial}{\partial\theta}-\mathrm{i}nq\right)r\frac{\partial x}{\partial r} + r\alpha_g'\left(\frac{\partial}{\partial\theta}-\mathrm{i}nq\right)y \\ &+ \alpha_g\left(\frac{\partial}{\partial\theta}-\mathrm{i}nq\right)\left[Q\frac{\partial x}{\partial\theta} - T\left(\frac{\partial}{\partial\theta}-\mathrm{i}nq\right)y - Uy\right] \\ &- \mathrm{i}nr\frac{\partial R^2}{\partial r}\alpha_p y + \mathrm{i}nR^2\alpha_p\left[T\left(\frac{\partial}{\partial\theta}-\mathrm{i}nq\right)y + Uy - Q\frac{\partial x}{\partial\theta}\right],\end{aligned} \tag{73}$$

which reduces to the *second outer-region p.d.e.*,[4]

$$\begin{aligned}\left(\frac{\partial}{\partial\theta}-\mathrm{i}nq\right)r\frac{\partial x}{\partial r} &= -\left(\frac{\partial}{\partial\theta}-\mathrm{i}nq\right)T^*\frac{\partial x}{\partial\theta} + U\frac{\partial x}{\partial\theta} + Xy \\ &- \left(\frac{\partial}{\partial\theta}-\mathrm{i}nq\right)V\left(\frac{\partial}{\partial\theta}-\mathrm{i}nq\right)y + W\left(\frac{\partial}{\partial\theta}-\mathrm{i}nq\right)y,\end{aligned} \tag{74}$$

where

$$V(r,\theta) = \frac{1}{|\nabla r|^2}\left(\frac{\mathrm{i}n}{R^2} + \frac{\alpha_g^2}{\mathrm{i}n}\right), \tag{75}$$

$$W(r,\theta) = \frac{2\alpha_g\alpha_p R^2}{|\nabla r|^2} - r\alpha_g', \tag{76}$$

$$X(r,\theta) = \mathrm{i}n\alpha_p\left[\frac{\partial}{\partial\theta}\left(T^* R^2\right) + r\frac{\partial R^2}{\partial r} - \alpha_f R^2 - U R^2\right], \tag{77}$$

and * denotes a complex conjugate.

IV. OUTER-REGION O.D.E.S

A. Primitive outer-region O.D.E.s

Let

$$x(r,\theta) = n z(r,\theta), \tag{78}$$

and let us express $y(r,\theta)$ and $z(r,\theta)$ as a Fourier series in the poloidal angle, θ:

$$y(r,\theta) = \sum_m y_m(r)\,\exp(\mathrm{i}m\theta), \tag{79}$$

$$z(r,\theta) = \sum_m z_m(r)\,\exp(\mathrm{i}m\theta). \tag{80}$$

Here, the (not necessarily positive) integers m are the poloidal mode numbers of the coupled Fourier harmonics included in the calculation. The outer-region p.d.e.s, (65) and (74), reduce to the *primitive outer-region o.d.e.s*,[4,6,16]

$$r\frac{d}{dr}\left[(m-nq)\,y_m\right] = \sum_{m'}\left(A_m^{m'} z_{m'} + B_m^{m'} y_{m'}\right), \tag{81}$$

$$(m-nq)\,r\frac{dz_m}{dr} = \sum_{m'}\left(C_m^{m'} z_{m'} + D_m^{m'} y_{m'}\right), \tag{82}$$

where

$$n^{-1}A_m^{m'}(r) = \frac{1}{2\pi\mathrm{i}}\oint \mathrm{e}^{-\mathrm{i}m\theta}\left(\frac{\partial}{\partial\theta}Q\frac{\partial}{\partial\theta} + S\right)\mathrm{e}^{\mathrm{i}m'\theta}\,d\theta, \tag{83}$$

$$B_m^{m'}(r) = \frac{1}{2\pi\mathrm{i}}\oint \mathrm{e}^{-\mathrm{i}m\theta}\left[-\frac{\partial}{\partial\theta}T\left(\frac{\partial}{\partial\theta}-\mathrm{i}nq\right) - \frac{\partial U}{\partial\theta}\right]\mathrm{e}^{\mathrm{i}m'\theta}\,d\theta, \tag{84}$$

$$C_m^{m'}(r) = \frac{1}{2\pi\mathrm{i}}\oint \mathrm{e}^{-\mathrm{i}m\theta}\left[-\left(\frac{\partial}{\partial\theta}-\mathrm{i}nq\right)T^*\frac{\partial}{\partial\theta} + U\frac{\partial}{\partial\theta}\right]\mathrm{e}^{\mathrm{i}m'\theta}\,d\theta, \tag{85}$$

$$nD_m^{m'}(r) = \frac{1}{2\pi\mathrm{i}}\oint \mathrm{e}^{-\mathrm{i}m\theta}\left[-\left(\frac{\partial}{\partial\theta}-\mathrm{i}nq\right)V\left(\frac{\partial}{\partial\theta}-\mathrm{i}nq\right) + W\left(\frac{\partial}{\partial\theta}-\mathrm{i}nq\right) + X\right]\mathrm{e}^{\mathrm{i}m'\theta}\,d\theta. \tag{86}$$

Hence, it follows from Eqs. (55)–(57), (64), and (75)–(77) that[16]

$$A_m^{m'} = m\,m'\,c_m^{m'} + n^2 r^2\,\delta_m^{m'}, \tag{87}$$

$$B_m^{m'} = m\,(m'-nq)\left(-f_m^{m'} + n^{-1}\alpha_g\,c_m^{m'}\right) - m\,\alpha_p\,d_m^{m'}, \tag{88}$$

$$C_m^{m'} = -(m-nq)\,m'\left(f_m^{m'} + n^{-1}\alpha_g\,c_m^{m'}\right) + m'\,\alpha_p\,d_m^{m'}, \tag{89}$$

$$D_m^{m'} = (m - n\,q)\,(m' - n\,q)\left(b_m^{m'} - n^{-2}\,\alpha_g^2\,c_m^{m'}\right) - (m - n\,q)\,n^{-1}\,r\,\alpha_g'\,\delta_m^{m'} + \alpha_p\left[(m - m')\,g_m^{m'} + n^{-1}\,\alpha_g\,(m + m' - 2\,n\,q)\,d_m^{m'} + r\,\frac{da_m^{m'}}{dr} - \alpha_f\,a_m^{m'} - \alpha_p\,e_m^{m'}\right], \tag{90}$$

where

$$a_m^{m'}(r) = \oint R^2\,\exp\left[-\mathrm{i}\,(m - m')\,\theta\right]\frac{d\theta}{2\pi}, \tag{91}$$

$$b_m^{m'}(r) = \oint |\nabla r|^{-2}\,R^{-2}\,\exp\left[-\mathrm{i}\,(m - m')\,\theta\right]\frac{d\theta}{2\pi}, \tag{92}$$

$$c_m^{m'}(r) = \oint |\nabla r|^{-2}\,\exp\left[-\mathrm{i}\,(m - m')\,\theta\right]\frac{d\theta}{2\pi}, \tag{93}$$

$$d_m^{m'}(r) = \oint |\nabla r|^{-2}\,R^2\,\exp\left[-\mathrm{i}\,(m - m')\,\theta\right]\frac{d\theta}{2\pi}, \tag{94}$$

$$e_m^{m'}(r) = \oint |\nabla r|^{-2}\,R^4\,\exp\left[-\mathrm{i}\,(m - m')\,\theta\right]\frac{d\theta}{2\pi}, \tag{95}$$

$$f_m^{m'}(r) = \oint \frac{\mathrm{i}\,r\,\nabla r\cdot\nabla\theta}{|\nabla r|^2}\,\exp\left[-\mathrm{i}\,(m - m')\,\theta\right]\frac{d\theta}{2\pi}, \tag{96}$$

$$g_m^{m'}(r) = \oint \frac{\mathrm{i}\,r\,\nabla r\cdot\nabla\theta}{|\nabla r|^2}\,R^2\,\exp\left[-\mathrm{i}\,(m - m')\,\theta\right]\frac{d\theta}{2\pi}. \tag{97}$$

Here, we have extended the analysis of Ref. 16, to take into account the fact that the $A_m^{m'}$, $B_m^{m'}$, $a_m^{m'}$, $b_m^{m'}$, etc., are complex quantities in a realistic non-up-down-symmetric tokamak plasma equilibrium. Note that $\delta_m^{m'}$ is a Kronecker delta symbol.

B. Outer-region O.D.E.s

Let

$$y_m(r) = \frac{\psi_m(r)}{m - n\,q}, \tag{98}$$

$$z_m(r) = \frac{Z_m(r) + k_m\,\psi_m(r)}{m - n\,q}, \tag{99}$$

where

$$k_m(r) = -\mathrm{Re}\left(\frac{B_m^m}{A_m^m}\right) = -\left[\frac{m\,(m - n\,q)\,n^{-1}\,\alpha_g\,c_m^m - m\,\alpha_p\,d_m^m}{m^2\,c_m^m + n^2\,r^2}\right]. \tag{100}$$

Here, we have made use of the fact that f_m^m is imaginary [see Eq. (96)]. It follows from Eq. (25) that

$$b^r(r,\theta) = \mathrm{i}\sum_m \frac{\psi_m(r)}{r\,R^2}\,\exp(\mathrm{i}\,m\,\theta). \tag{101}$$

Furthermore, Eqs. (81) and (82) transform to give the *outer-region o.d.e.s*,[6,16]

$$r\,\frac{d\psi_m}{dr} = \sum_{m'}\frac{L_m^{m'}\,Z_{m'} + M_m^{m'}\,\psi_{m'}}{m' - n\,q}, \tag{102}$$

$$(m - n\,q)\,r\,\frac{d}{dr}\left(\frac{Z_m}{m - n\,q}\right) = \sum_{m'}\frac{N_m^{m'}\,Z_{m'} + P_m^{m'}\,\psi_{m'}}{m' - n\,q}, \tag{103}$$

where

$$L_m^{m'}(r) = A_m^{m'}, \tag{104}$$

$$M_m^{m'}(r) = B_m^{m'} + k_{m'}\,L_m^{m'}, \tag{105}$$

$$N_m^{m'}(r) = C_m^{m'} - k_m\,L_m^{m'}, \tag{106}$$

$$P_m^{m'}(r) = D_m^{m'} + k_{m'}\,C_m^{m'} - k_m\,M_m^{m'} - k_m\,n\,q\,s\,\delta_m^{m'} - (m - n\,q)\,r\,\frac{dk_m}{dr}\,\delta_m^{m'}, \tag{107}$$

with

$$s(r) = \frac{r\,q'}{q}. \tag{108}$$

Note that

$$M_m^m = N_m^m = -m\,(m - n\,q)\,f_m^m. \tag{109}$$

C. Symmetry properties of coupling matrices

Equations (91)–(97) imply that $a_{m'}^m = a_m^{m'*}$, $b_{m'}^m = b_m^{m'*}$, $c_{m'}^m = c_m^{m'*}$, $d_{m'}^m = d_m^{m'*}$, $e_{m'}^m = e_m^{m'*}$, $f_{m'}^m = -f_m^{m'*}$, and $g_{m'}^m = -g_m^{m'*}$, for all m, m'. Hence, Eqs. (87)–(90), (100), and (104)–(107) give

$$L_{m'}^m = L_m^{m'*}, \tag{110}$$

$$M_{m'}^m = -N_m^{m'*}, \tag{111}$$

$$N_{m'}^m = -M_m^{m'*}, \tag{112}$$

$$P_{m'}^m = P_m^{m'*}, \tag{113}$$

for all m, m'.

D. Toroidal electromagnetic torque

The volume-integrated toroidal electromagnetic torque acting between the magnetic axis and a magnetic flux surface whose label is r is given by

$$T_\phi(r) = \int_0^r \oint\oint R^2\,\nabla\phi\cdot(\mathbf{J} + \mathbf{j})\times(\mathbf{B} + \mathbf{b})\,\mathcal{J}\,d\tilde{r}\,d\theta\,d\phi = \int_0^r \oint\oint (\mathbf{j}\times\mathbf{b})_\phi\,\mathcal{J}\,d\tilde{r}\,d\theta\,d\phi. \tag{114}$$

Here, use has been made of Eq. (14), as well as the fact that $P = P(r)$. We have also taken into account that $\mathbf{b}$ and $\mathbf{j}$ vary with ϕ as $\exp(-\mathrm{i}\,n\,\phi)$, whereas $\mathbf{B}$, $\mathbf{J}$, $\mathcal{J}$, and $|\nabla\phi|$ are independent of ϕ. It is clear that the zeroth-order (in perturbed quantities) contribution to T_ϕ is identically zero, whereas the first-order contributions average to zero, leaving only second-order (i.e., nonlinear in perturbed quantities) contributions. Making use of the Appendix, as well as Eqs. (2), (20), (50), (53), and (62), we deduce that

$$\mathcal{J}\,(\mathbf{j}\times\mathbf{b})_\phi = \frac{\partial}{\partial r}\left(\mathcal{J}\,b_\phi\,b^r\right) + \frac{\partial}{\partial\theta}\left(\mathcal{J}\,b_\phi\,b^\theta\right) + \frac{\partial}{\partial\phi}\left(\mathcal{J}\,b_\phi\,b^\phi\right) - \frac{1}{2}\,\frac{\partial}{\partial\phi}\left[\mathcal{J}\left(b_r\,b^r + b_\theta\,b^\theta + b_\phi\,b^\phi\right)\right]. \tag{115}$$

Hence, we obtain

$$T_\phi(r) = \oint\oint\int \mathcal{J}\, b_\phi\, b^r\, d\theta\, d\phi = r \oint\oint\int R^2\, b_\phi\, b^r\, d\theta\, d\phi, \tag{116}$$

where the integral on the right-hand side is evaluated on the magnetic flux surface whose label is r. We can reinterpret the previous expression as specifying the net outward flux of toroidal electromagnetic angular momentum across the magnetic flux surface whose label is r. Finally, making use of Eqs. (47), (78), (80), and (99)–(101), the previous expression reduces to[6]

$$T_\phi(r) = \mathrm{i}\,\pi^2\, n \sum_m \frac{Z_m^*\,\psi_m - \psi_m^*\,Z_m}{m - n\,q}. \tag{117}$$

It follows from Eqs. (102), (103), and (110)–(113) that

$$r\,\frac{d}{dr}\left(\sum_m \frac{Z_m^*\,\psi_m - \psi_m^*\,Z_m}{m - n\,q}\right) = 0. \tag{118}$$

Hence, we deduce that[6]

$$\frac{dT_\phi}{dr} = 0 \tag{119}$$

in any region of the plasma that satisfies the outer-region o.d.e.s. Thus, the volume-integrated toroidal electromagnetic torque acting between the magnetic axis and a given magnetic flux surface is constant between rational magnetic flux surfaces. As will become apparent in Sec. V D, the integrated torque can have discontinuous jumps across rational flux surfaces. It follows that net electromagnetic torques can only develop in the plasma in the immediate vicinity of rational magnetic flux surfaces, where the ideal MHD equations become singular.[28]

V. BEHAVIOR IN VICINITY OF RATIONAL SURFACE

A. Introduction

The analysis of this section is a generalization of the analysis of Ref. 16 that takes into account the fact that the $L_m^{m'}$, $M_m^{m'}$, etc., are complex quantities in a realistic non-up-down-symmetric tokamak plasma equilibrium.

Let there be K rational magnetic flux surfaces in the plasma. Suppose that the kth surface lies at $r = r_k$ and possesses the resonant poloidal mode number m_k, where $q(r_k) = m_k/n$.

B. General case

Consider the solution of the outer-region o.d.e.s, (102) and (103), in the vicinity of the kth rational surface. Let $x = r - r_k$. The most general small-$|x|$ solution of the o.d.e.s can be shown to take the form[6,16]

$$\psi_{m_k}(r_k + x) = A_{Lk}^{\pm}\,|x|^{\nu_{L\,k}}\,(1 + \lambda_L\,x + \cdots) + A_{Sk}^{\pm}\,\mathrm{sgn}(x)\,|x|^{\nu_{S\,k}}\,(1 + \cdots) + A_C\,x\,(1 + \cdots), \tag{120}$$

$$Z_{m_k}(r_k + x) = A_{Lk}^{\pm}\,|x|^{\nu_{L\,k}}(b_L + \gamma_L\,x + \cdots) + A_{Sk}^{\pm}\,\mathrm{sgn}(x)\,|x|^{\nu_{S\,k}}\,(b_S + \cdots) + B_C\,x\,(1 + \cdots), \tag{121}$$

and

$$\psi_{m_k+j}(r_k + x) = A_{Lk}^{\pm}\,|x|^{\nu_{L\,k}}\,(a_j + c_j\,x + \cdots) + A_{Sk}^{\pm}\,\mathrm{sgn}(x)\,|x|^{\nu_{S\,k}} \times\,(\tilde{a}_j + \cdots) + (\bar{\psi}_{m_k+j} + \bar{\psi}'_{m_j+k}\,x + \cdots), \tag{122}$$

$$Z_{m_k+j}(r_k + x) = A_{Lk}^{\pm}\,|x|^{\nu_{L\,k}}\,(b_j + d_j\,x + \cdots) + A_{Sk}^{\pm}\,\mathrm{sgn}(x)\,|x|^{\nu_{S\,k}} \times\,(\tilde{b}_j + \cdots) + (\bar{Z}_{m_k+j} + \bar{Z}'_{m_k+j}\,x + \cdots), \tag{123}$$

for $j \neq 0$. The superscripts $^+$ and $^-$ correspond to $x > 0$ and $x < 0$, respectively. Here, A_{Lk} is known as the "coefficient of the large solution," whereas A_{Sk} is termed the "coefficient of the small solution."[6,16,29] Moreover,

$$\nu_{Lk} = \frac{1}{2} - \sqrt{-D_{Ik}}, \tag{124}$$

$$\nu_{Sk} = \frac{1}{2} + \sqrt{-D_{Ik}}, \tag{125}$$

$$D_{Ik} = -L_0\,P_0 - \frac{1}{4}, \tag{126}$$

$$L_0 = -\left(\frac{L_{m_k}^{m_k}}{m_k\,s}\right)_{r_k}, \tag{127}$$

$$P_0 = -\left(\frac{P_{m_k}^{m_k}}{m_k\,s}\right)_{r_k}. \tag{128}$$

Note that, ordinarily, ν_{Lk}, ν_{Sk}, D_{Ik}, L_0, and P_0 are all real quantities. Furthermore,

$$b_L = \frac{\nu_{Lk}}{L_0}, \tag{129}$$

$$b_S = \frac{\nu_{Sk}}{L_0}, \tag{130}$$

$$A_C = -\frac{1}{r_k\,P_0}\sum_{j\neq 0}\frac{1}{j}\left(N_{m_k}^{m_k+j}\,\bar{Z}_{m_k+j} + P_{m_k}^{m_k+j}\,\bar{\psi}_{m_k+j}\right)_{r_k}, \tag{131}$$

$$B_C = -\frac{1}{r_k\,L_0}\sum_{j\neq 0}\frac{1}{j}\left(L_{m_k}^{m_k+j}\,\bar{Z}_{m_k+j} + M_{m_k}^{m_k+j}\,\bar{\psi}_{m_k+j}\right)_{r_k} + \frac{A_C}{L_0}, \tag{132}$$

$$\lambda_L = \frac{1}{2\,r_k}\left[\frac{P_1\,L_0}{\nu_{Lk}} + T_1 + \nu_{Lk}\left(\frac{L_1}{L_0} - 2\right) + 2\,M_1\right]_{r_k} - \frac{1}{2\,(m_k\,s)_{r_k}}\,\frac{1}{r_k\,\nu_{Lk}} \times\sum_{j\neq 0}\frac{1}{j}\left[L_{m_k}^{m_k+j}\,P_{m_k+j}^{m_k} + P_{m_k}^{m_k+j}\,L_{m_k+j}^{m_k} + M_{m_k}^{m_k+j}\,M_{m_k+j}^{m_k} + N_{m_k}^{m_k+j}\,N_{m_k+j}^{m_k} + b_L\,(L_{m_k}^{m_k+j}\,N_{m_k+j}^{m_k} + M_{m_k}^{m_k+j}\,L_{m_k+j}^{m_k}) + \frac{1}{b_L}\,(N_{m_k}^{m_k+j}\,P_{m_k+j}^{m_k} + P_{m_k}^{m_k+j}\,M_{m_k+j}^{m_k})\right]_{r_k}, \tag{133}$$

$$\gamma_L = \frac{1}{2\,r_k}\left[(1+\nu_{Lk})\left(\frac{P_1}{\nu_{Lk}} + \frac{T_1}{L_0} - \frac{\nu_{Lk}}{L_0}\right) + P_0\left(\frac{L_1}{L_0} - 1\right) + 2\,b_L\,M_1\right]_{r_k} - \frac{1}{2\,(m_k\,s)_{r_k}}\,\frac{1}{r_k\,\nu_{Lk}\,L_0}\sum_{j\neq 0}\frac{1}{j}\left[(\nu_{Lk}+1)\,(P_{m_k}^{m_k+j}\,L_{m_k+j}^{m_k} + N_{m_k}^{m_k+j}\,N_{m_k+j}^{m_k}) + (\nu_{Lk}-1)\,(L_{m_k}^{m_k+j}\,P_{m_k+j}^{m_k} + M_{m_k}^{m_k+j}\,M_{m_k+j}^{m_k}) + b_L\,(\nu_{Lk}-1)\,(L_{m_k}^{m_k+j}\,N_{m_k+j}^{m_k} + M_{m_k}^{m_k+j}\,L_{m_k+j}^{m_k}) + \frac{1}{b_L}\left(\nu_{Lk}+1\right)(N_{m_k}^{m_k+j}\,P_{m_k+j}^{m_k} + P_{m_k}^{m_k+j}\,M_{m_k+j}^{m_k})\right]_{r_k}, \tag{134}$$

$$a_j = -\frac{1}{(m_k\, s)_{r_k}}\left(\frac{L^{m_k}_{m_k+j}}{L_0}+\frac{M^{m_k}_{m_k+j}}{\nu_{Lk}}\right)_{r_k}, \tag{135}$$

$$b_j = -\frac{1}{(m_k\, s)_{r_k}}\left(\frac{P^{m_k}_{m_k+j}}{\nu_{Lk}}+\frac{N^{m_k}_{m_k+j}}{L_0}\right)_{r_k}, \tag{136}$$

$$\tilde{a}_j = -\frac{1}{(m_k\, s)_{r_k}}\left(\frac{L^{m_k}_{m_k+j}}{L_0}+\frac{M^{m_k}_{m_k+j}}{\nu_{Sk}}\right)_{r_k}, \tag{137}$$

$$\tilde{b}_j = -\frac{1}{(m_k\, s)_{r_k}}\left(\frac{P^{m_k}_{m_k+j}}{\nu_{Sk}}+\frac{N^{m_k}_{m_k+j}}{L_0}\right)_{r_k}, \tag{138}$$

$$c_j = \frac{1}{(1+\nu_{Lk})\, r_k}\left[-\nu_{Lk}\, a_j + L_{j1}\, b_L + M_{j1} - \frac{r_k}{m_k\, s}\left(L^{m_k}_{m_k+j}\,\gamma_L + M^{m_k}_{m_k+j}\,\lambda_L\right) + \sum_{j'\neq 0}\frac{1}{j'}\left(L^{m_k+j'}_{m_k+j}\, b_{j'} + M^{m_k+j'}_{m_k+j}\, a_{j'}\right)\right]_{r_k}, \tag{139}$$

$$d_j = \frac{1}{(1+\nu_{Lk})\, r_k}\left[-\left(\nu_{Lk}+\frac{m_k\, s}{j}\right) b_j + N_{j1}\, b_L + P_{j1} - \frac{r_k}{m_k\, s}\left(N^{m_k}_{m_k+j}\,\gamma_L + P^{m_k}_{m_k+j}\,\lambda_L\right) + \sum_{j'\neq 0}\frac{1}{j'}\left(N^{m_k+j'}_{m_k+j}\, b_{j'} + P^{m_k+j'}_{m_k+j}\, a_{j'}\right)\right]_{r_k}, \tag{140}$$

$$\bar{\psi}_{m_k+j'} = \frac{1}{r_k}\left[-\frac{r_k}{m_k\, s}\left(L^{m_k}_{m_k+j}\, B_C + M^{m_k}_{m_k+j}\, A_C\right) + \sum_{j'\neq 0}\frac{1}{j'}\left(L^{m_k+j'}_{m_k+j}\,\bar{Z}_{m_k+j'} + M^{m_k+j'}_{m_k+j}\,\bar{\psi}_{m_k+j'}\right)\right]_{r_k}, \tag{141}$$

$$\bar{Z}_{m_k+j'} = \frac{1}{r_k}\left[-\frac{m_k\, s}{j}\,\bar{Z}_{m_k+j} - \frac{r_k}{m_k\, s}\left(N^{m_k}_{m_k+j}\, B_C + P^{m_k}_{m_k+j}\, A_C\right) + \sum_{j'\neq 0}\frac{1}{j'}\left(N^{m_k+j'}_{m_k+j}\,\bar{Z}_{m_k+j'} + P^{m_k+j'}_{m_k+j}\,\bar{\psi}_{m_k+j'}\right)\right]_{r_k}, \tag{142}$$

and

$$L_1 = \lim_{x\to 0}\left(\frac{L^{m_k}_{m_k}}{m_k - n\, q} - \frac{r_k\, L_0}{x}\right), \tag{143}$$

$$P_1 = \lim_{x\to 0}\left(\frac{P^{m_k}_{m_k}}{m_k - n\, q} - \frac{r_k\, P_0}{x}\right), \tag{144}$$

$$T_1 = \lim_{x\to 0}\left(\frac{-n\, q\, s}{m_k - n\, q} - \frac{r_k}{x}\right), \tag{145}$$

$$M_1 = \lim_{x\to 0}\left(\frac{M^{m_k}_{m_k}}{m_k - n\, q}\right), \tag{146}$$

$$L_{j1} = \lim_{x\to 0}\left(\frac{L^{m_k}_{m_k+j}}{m_k - n\, q} + \frac{r_k}{m_k\, s}\,\frac{L^{m_k}_{m_k+j}}{x}\right), \tag{147}$$

$$M_{j1} = \lim_{x\to 0}\left(\frac{M^{m_k}_{m_k+j}}{m_k - n\, q} + \frac{r_k}{m_k\, s}\,\frac{M^{m_k}_{m_k+j}}{x}\right), \tag{148}$$

$$N_{j1} = \lim_{x\to 0}\left(\frac{N^{m_k}_{m_k+j}}{m_k - n\, q} + \frac{r_k}{m_k\, s}\,\frac{N^{m_k}_{m_k+j}}{x}\right), \tag{149}$$

$$P_{j1} = \lim_{x\to 0}\left(\frac{P^{m_k}_{m_k+j}}{m_k - n\, q} + \frac{r_k}{m_k\, s}\,\frac{P^{m_k}_{m_k+j}}{x}\right), \tag{150}$$

where $j \neq 0$.

The coefficients of the large and the small solutions at the kth rational surface are evaluated as follows:

$$\bar{\psi}_{m_k+j} = \psi_{m_k+j}(r_k+\delta) - (a_j + \delta\, c_j)\, A_{Lk}\, |\delta|^{\nu_{L\,k}} - \tilde{a}_j\, \mathrm{sgn}(\delta)\, A_{Sk}\, |\delta|^{\nu_{S\,k}} - \bar{\psi}'_{m_k+j}\,\delta + \mathcal{O}(\delta^2), \tag{151}$$

$$\bar{Z}_{m_k+j} = Z_{m_k+j}(r_k+\delta) - (b_j + \delta\, d_j)\, A_{Lk}\, |\delta|^{\nu_{L\,k}} - \tilde{b}_j\, \mathrm{sgn}(\delta)\, A_{Sk}\, |\delta|^{\nu_{S\,k}} - \bar{Z}'_{m_k+j}\,\delta + \mathcal{O}(\delta^2), \tag{152}$$

$$A_{Sk} = \frac{Z_{m_k}(r_k+\delta) - b_L\,\psi_{m_k}(r_k+\delta) - \delta\,(B_C - b_L\, A_C) - \delta\,(\gamma_L - b_L\,\lambda_L)\, A_{Lk}\, |\delta|^{\nu_{L\,k}}}{(b_S - b_L)\,\mathrm{sgn}(\delta)\, |\delta|^{\nu_{S\,k}}} + \mathcal{O}(\delta), \tag{153}$$

$$A_{Lk} = \frac{\psi_{m_k}(r_k+\delta) - A_{Sk}\,\mathrm{sgn}(\delta)\, |\delta|^{\nu_{S\,k}} - A_C\,\delta}{(1+\delta\,\lambda_L)\, |\delta|^{\nu_{L\,k}}} + \mathcal{O}(\delta^2), \tag{154}$$

for $j \neq 0$. The previous set of equations can be solved via iteration. Here, $\delta \ll 1$ is a numerical parameter that controls how close the outer-region o.d.e. solutions are allowed to approach the various rational surfaces in the plasma. If the asymptotic matching procedure is working correctly, then the coefficients of the large and small solutions should exhibit no dependance on δ, once it falls below a critical value. In this situation, the procedure is deemed to have converged.

Note that the analysis in this section is based on the assumption that $D_{Ik} < 0$. If $D_{Ik} > 0$, then the indices ν_{Lk} and ν_{Sk} become complex, indicating that the plasma in the vicinity of the kth rational surface is unstable to localized ideal interchange modes.[30]

C. Special case

In the limit $\nu_{Lk} \to 0$, some of the previous expressions become singular, and a special treatment is required. Such a special treatment is always needed for rational surfaces characterized by $q = 1$. The most general small-$|x|$ solution of the outer-region o.d.e.s takes the form

$$\psi_{m_k}(r_k + x) = A^{\pm}_{Lk}\left[1 + \nu_{Lk}\,\ln|x| + \hat{\lambda}_L\,x\,(\ln|x| - 1) + \mu_L\,x\,(\ln^2|x| - 2\,\ln|x| + 2) + \xi_L\,x + \cdots\right] + A^{\pm}_{Sk}\,x\,(1 + \cdots) + \hat{A}_C\,x\,(1 + \cdots) + A_D\,x\,(\ln|x| - 1 + \cdots), \tag{155}$$

$$Z_{m_k}(r_k + x) = A^{\pm}_{Lk}\left(b_L + \hat{\gamma}_L\,x\,\ln|x| + \delta_L\,x\,\ln^2|x| + \cdots\right) + A^{\pm}_{Sk}\,x\,(b_S + \cdots) + B_D\,x\,(\ln|x| + \cdots), \tag{156}$$

and

$$\psi_{m_k+j}(r_k + x) = A^{\pm}_{Lk}\left[\hat{a}_j\,\ln|x| + x\,(\hat{c}_j + \hat{c}'_j\,\ln|x| + \hat{c}''_j\,\ln^2|x|) + \cdots\right] + A^{\pm}_{Sk}\,x\,(\tilde{a}_j + \cdots) + \left[\bar{\psi}_{m_k+j} + x\,(\bar{\psi}''_{m_k+j} + \bar{\psi}'''_{m_k+j}\,\ln|x| \cdots)\right], \tag{157}$$

$$Z_{m_k+j}(r_k + x) = A^{\pm}_{Lk}\left[\hat{b}_j\,\ln|x| + x\,(\hat{d}_j + \hat{d}'_j\,\ln|x| + \hat{d}''_j\,\ln^2|x|) + \cdots\right] + A^{\pm}_{Sk}\,x\,(\tilde{b}_j + \cdots) + \left[\bar{Z}_{m_k+j} + x\,(\bar{Z}''_{m_k+j} + \bar{Z}'''_{m_k+j}\,\ln|x| \cdots)\right], \tag{158}$$

for $j \neq 0$. Here,

$$\hat{A}_C = \frac{1}{r_k}\sum_{j\neq 0}\frac{1}{j}\left(L^{m_k+j}_{m_k}\,\bar{Z}_{m_k+j} + M^{m_k+j}_{m_k}\,\bar{\psi}_{m_k+j}\right)_{r_k}, \tag{159}$$

$$A_D = \frac{L_0}{r_k}\sum_{j\neq 0}\frac{1}{j}\left(N^{m_k+j}_{m_k}\,\bar{Z}_{m_k+j} + P^{m_k+j}_{m_k}\,\bar{\psi}_{m_k+j}\right)_{r_k} - \nu_{Lk}\,\hat{A}_C, \tag{160}$$

$$B_D = \frac{A_D}{L_0}, \tag{161}$$

$$\hat{\lambda}_L = \frac{P_1\,L_0\,(1 + \nu_{Lk})}{r_k} + \frac{\nu_{Lk}\,T_1}{r_k} - \frac{1}{(m_k\,s)_{r_k}}\frac{1}{r_k}\sum_{j\neq 0}\frac{1}{j}\left(L^{m_k+j}_{m_k}\,P^{m_k}_{m_k+j} + M^{m_k+j}_{m_k}\,M^{m_k}_{m_k+j}\right)_{r_k} - \frac{1}{(m_k\,s)_{r_k}}\frac{\nu_{Lk}}{L_0\,r_k}\left(L^{m_k+j}_{m_k}\,N^{m_k}_{m_k+j} + M^{m_k+j}_{m_k}\,L^{m_k}_{m_k+j}\right)_{r_k}, \tag{162}$$

$$\mu_L = -\frac{1}{2\,(m_k\,s)_{r_k}}\frac{L_0}{r_k}\sum_{j\neq 0}\frac{1}{j}\,(N^{m_k+j}_{m_k}\,P^{m_k}_{m_k+j} + P^{m_k+j}_{m_k}\,M^{m_k}_{m_k+j})_{r_k}, \tag{163}$$

$$\xi_L = M_1 + \frac{\nu_{Lk}}{r_k}\left(\frac{L_1}{L_0} - 1\right), \tag{164}$$

$$\hat{\gamma}_L = \frac{P_1\,(1 + \nu_{Lk})}{r_k} + \frac{\nu_{Lk}\,T_1}{L_0\,r_k}, \tag{165}$$

$$\delta_L = \frac{\mu_L}{L_0}, \tag{166}$$

$$\hat{a}_j = -\frac{1}{(m_k\,s)_{r_k}}\left(\frac{\nu_{Lk}\,L^{m_k}_{m_k+j}}{L_0} + M^{m_k}_{m_k+j}\right)_{r_k}, \tag{167}$$

$$\hat{b}_j = -\frac{1}{(m_k\,s)_{r_k}}\left(P^{m_k}_{m_k+j} + \frac{\nu_{Lk}\,N^{m_k}_{m_k+j}}{L_0}\right)_{r_k}, \tag{168}$$

$$\hat{c}_j = \frac{1}{r_k}\left\{-\hat{a}_j + L_{j1}\,b_L + M_{j1}\,(1 - \nu_{Lk}) + \frac{r_k}{m_k\,s}\left[L^{m_k}_{m_k+j}\,(\hat{\gamma}_L - 2\,\delta_L) + M^{m_k}_{m_k+j}\,(2\,\hat{\lambda}_L - 6\,\mu_L - \xi_L)\right] - \sum_{j'\neq 0}\frac{1}{j'}\left(L^{m_k+j'}_{m_k+j}\,\hat{b}_{j'} + M^{m_k+j'}_{m_k+j}\,\hat{a}_{j'}\right)\right\}_{r_k}, \tag{169}$$

$$\hat{c}'_j = \frac{1}{r_k}\left\{M_{j1}\,\nu_{Lk} - \frac{r_k}{m_k\,s}\left[L^{m_k}_{m_k+j}\,(\hat{\gamma}_L - 2\,\delta_L) + M^{m_k}_{m_k+j}\,(\hat{\lambda}_L - 4\,\mu_L)\right] + \sum_{j'\neq 0}\frac{1}{j'}\left(L^{m_k+j'}_{m_k+j}\,\hat{b}_{j'} + M^{m_k+j'}_{m_k+j}\,\hat{a}_{j'}\right)\right\}_{r_k}, \tag{170}$$

$$\hat{c}''_j = \frac{1}{r_k}\left[-\frac{r_k}{m_k\,s}\left(L^{m_k+j'}_{m_k+j}\,\delta_L + M^{m_k+j'}_{m_k+j}\,\mu_L\right)\right]_{r_k}, \tag{171}$$

$$\hat{d}_j = \frac{1}{r_k}\left\{-\left(1-\frac{m_k\,s}{j}\right)\hat{b}_j + N_{j1}\,b_L + P_{j1}\,(1-\nu_{Lk}) + \frac{r_k}{m_k\,s}[N^{m_k}_{m_k+j}\,(\hat{\gamma}_L - 2\,\delta_L) + P^{m_k}_{m_k+j}\,(2\,\hat{\lambda}_L - 6\,\mu_L - \xi_L)] - \sum_{j'\neq 0}\frac{1}{j'}\left(N^{m_k+j'}_{m_k+j}\,\hat{b}_{j'} + P^{m_k+j'}_{m_k+j}\,\hat{a}_{j'}\right)\right\}_{r_k}, \tag{172}$$

$$\hat{d}'_j = \frac{1}{r_k}\left\{-\frac{m_k\,s}{j}\,\hat{b}_j + P_{j1}\,\nu_{Lk} - \frac{r_k}{m_k\,s}[N^{m_k}_{m_k+j}\,(\hat{\gamma}_L - 2\,\delta_L) + P^{m_k}_{m_k+j}\,(\hat{\lambda}_L - 4\,\mu_L)] + \sum_{j'\neq 0}\frac{1}{j'}\left(N^{m_k+j'}_{m_k+j}\,\hat{b}_{j'} + P^{m_k+j'}_{m_k+j}\,\hat{a}_{j'}\right)\right\}_{r_k}, \tag{173}$$

$$\hat{d}''_j = \frac{1}{r_k}\left[-\frac{r_k}{m_k\,s}\,(N^{m_k+j'}_{m_k+j}\,\delta_L + P^{m_k+j'}_{m_k+j}\,\mu_L)\right]_{r_k}, \tag{174}$$

$$\bar{\psi}''_{m_k+j} = \frac{1}{r_k}\left\{-\frac{r_k}{m_k\,s}[-L^{m_k}_{m_k+j}\,B_D + M^{m_k}_{m_k+j}\,(\hat{A}_C - 2\,A_D)] + \sum_{j'\neq 0}\frac{1}{j'}\left(L^{m_k+j'}_{m_k+j}\,\bar{Z}_{m_k+j'} + M^{m_k+j'}_{m_k+j}\,\bar{\psi}_{m_k+j'}\right)\right\}_{r_k}, \tag{175}$$

$$\bar{\psi}'''_{m_k+j} = \frac{1}{r_k}\left[-\frac{r_k}{m_k\,s}\left(L^{m_k}_{m_k+j}\,B_D + M^{m_k}_{m_k+j}\,A_D\right)\right]_{r_k}, \tag{176}$$

$$\bar{Z}''_{m_k+j} = \frac{1}{r_k}\left\{-\frac{m_k\,s}{j}\,\bar{Z}_{m_k+j} - \frac{r_k}{m_k\,s}[-N^{m_k}_{m_k+j}\,B_D + P^{m_k}_{m_k+j}\,(\hat{A}_C - 2\,A_D)] + \sum_{j'\neq 0}\frac{1}{j'}\left(N^{m_k+j'}_{m_k+j}\,\bar{Z}_{m_k+j'} + P^{m_k+j'}_{m_k+j}\,\bar{\psi}_{m_k+j'}\right)\right\}_{r_k}, \tag{177}$$

$$\bar{Z}'''_{m_k+j} = \frac{1}{r_k}\left[-\frac{r_k}{m_k\,s}\left(N^{m_k}_{m_k+j}\,B_D + P^{m_k}_{m_k+j}\,A_D\right)\right]_{r_k}. \tag{178}$$

Moreover, $\tilde{a}_j$ and $\tilde{b}_j$ are again specified by Eqs. (137) and (138).

The coefficients of the large and the small solutions at the kth rational surface are evaluated as follows:

$$\bar{\psi}_{m_k+j} = \psi_{m_k+j}(r_k+\delta) - \left[\hat{a}_j\,\ln|\delta| + \delta\,(\hat{c}_j + \hat{c}'_j\,\ln|\delta| + \hat{c}''_j\,\ln^2|\delta|)\right]A_{Lk} - \tilde{a}_j\,A_{Sk}\,\delta - (\bar{\psi}''_{m_k+j} + \bar{\psi}'''_{m_k+j}\,\ln|\delta|)\,\delta + \mathcal{O}(\delta^2), \tag{179}$$

$$\bar{Z}_{m_k+j} = Z_{m_k+j}(r_k+\delta) - \left[\hat{b}_j\,\ln|\delta| + \delta\,(\hat{d}_j + \hat{d}_{j'}\,\ln|\delta| + \hat{d}_{j''}\,\ln^2|\delta|)\right]A_{Lk} - \tilde{b}_j\,A_{Sk}\,\delta - (\bar{Z}''_{m_k+j} + \bar{Z}'''_{m_k+j}\,\ln|\delta|)\,\delta + \mathcal{O}(\delta^2), \tag{180}$$

$$A_{Sk} = \frac{Z_{m_k}(r_k+\delta) - b_L\,A_{Lk} - \delta\,\ln|\delta|\,[B_D + (\hat{\gamma}_L + \delta_L\,\ln|\delta|)\,A_{Lk}]}{b_S\,\delta} + \mathcal{O}(\delta), \tag{181}$$

$$A_{Lk} = \frac{\psi_{m_k}(r_k+\delta) - \delta\left[A_{Sk} + \hat{A}_C + A_D\,(\ln|\delta| - 1)\right]}{1 + \nu_{Lk}\,\ln|\delta| + \delta\left[\hat{\lambda}_L\,(\ln|\delta| - 1) + \mu_L\,(\ln^2|\delta| - 2\,\ln|\delta| + 2) + \xi_L\right]} + \mathcal{O}(\delta^2), \tag{182}$$

for $j \neq 0$. As before, the previous equations can be solved via iteration (see the discussion of the numerical parameter δ in Sec. V B).

D. Asymptotic matching across rational surfaces

Consider the resonant layer solution in the vicinity of the kth rational surface, whose resonant poloidal mode number is m_k. This solution can be separated into independent tearing and twisting parity components.[29] The tearing parity component is such that $\psi_{m_k}(r_k - x) = \psi_{m_k}(r_k + x)$ throughout the layer, whereas the twisting parity component is such that $\psi_{m_k}(r_k - x) = -\psi_{m_k}(r_k + x)$. It turns out, however, that the twisting parity response of a resonant layer to the solution in the outer region is generally negligible compared to the tearing parity response.[4,16,31] Hence, in this paper, we shall neglect the twisting parity responses of the various resonant layers in the plasma all together.

The neglect of the twisting parity responses of the various resonant layers in the plasma implies that the coefficients of the large solution to the left and to the right of each rational surface in the plasma are equal to one another.[6] In other words,

$$A^-_{Lk} = A^+_{Lk} = A_{Lk}, \tag{183}$$

for all k. Note, however, that the coefficients of the small solution to the left and to the right of a given rational surface are not, in general, equal to one another.

Consider a solution that is completely continuous across the kth rational surface, so that $A^-_{Sk} = A^+_{Sk}$. According to the preceding analysis, the continuity conditions for the various poloidal harmonics can be written as

$$\psi_{m_k}(r_k + |\delta|) = \psi_{m_k}(r_k - |\delta|) + 2\,|\delta|\,\left[A_{Lk}\,|\delta|^{\nu_{L\,k}}\,\lambda_L + A_C\right] + 2\,A^-_{Sk}\,|\delta|^{\nu_{S\,k}} + \mathcal{O}(\delta^2), \tag{184}$$

$$Z_{m_k}(r_k + |\delta|) = Z_{m_k}(r_k - |\delta|) + 2\,|\delta|\,\left[A_{Lk}\,|\delta|^{\nu_{L\,k}}\,\gamma_L + B_C\right] + 2\,A^-_{Sk}\,b_S\,|\delta|^{\nu_{S\,k}} + \mathcal{O}(\delta^2), \tag{185}$$

$$\psi_{m_k+j}(r_k+|\delta|) = \psi_{m_k+j}(r_k-|\delta|) + 2\,|\delta|\left[A_{Lk}\,|\delta|^{\nu_{L\,k}}\,c_j + \bar{\psi}'_{m_k+j}\right] + 2\,A^-_{Sk}\,\tilde{a}_j\,|\delta|^{\nu_{S\,k}} + \mathcal{O}(\delta^2), \tag{186}$$

$$Z_{m_k+j}(r_k+|\delta|) = Z_{m_k+j}(r_k-|\delta|) + 2\,|\delta|\left[A_{Lk}\,|\delta|^{\nu_{L\,k}}\,d_j + \bar{Z}'_{m_k+j}\right] + 2\,A^-_{Sk}\,\tilde{b}_j\,|\delta|^{\nu_{S\,k}} + \mathcal{O}(\delta^2), \tag{187}$$

in the general case, and

$$\psi_{m_k}(r_k+|\delta|) = \psi_{m_k}(r_k-|\delta|) + 2\,|\delta|\left\{A_{Lk}\left[\hat{\lambda}_L\,(\ln|\delta|-1) + \hat{\mu}_L\,(\ln^2|\delta| - 2\,\ln|\delta| + 2) + \xi_L\right] + \hat{A}_C + A_D\,(\ln|\delta|-1) + A^-_{Sk}\right\} + \mathcal{O}(\delta^2), \tag{188}$$

$$Z_{m_k}(r_k+|\delta|) = Z_{m_k}(r_k-|\delta|) + 2\,|\delta|\,[A_{Lk}\,\ln|\delta|\,(\hat{\gamma}_L + \delta_L\,\ln|\delta|) + B_D\,\ln|\delta| + A^-_{Sk}\,b_S] + \mathcal{O}(\delta^2), \tag{189}$$

$$\psi_{m_k+j}(r_k+|\delta|) = \psi_{m_k+j}(r_k-|\delta|) + 2\,|\delta|[A_{Lk}\,(\hat{c}_j + \hat{c}'_j\,\ln|\delta| + \hat{c}''_j\,\ln^2|\delta|) + A^-_{Sk}\,\tilde{a}_j + \bar{\psi}''_{m_k+j} + \bar{\psi}'''_{m_k+j}\,\ln|\delta|] + \mathcal{O}(\delta^2), \tag{190}$$

$$Z_{m_k+j}(r_k+|\delta|) = Z_{m_k+j}(r_k-|\delta|) + 2\,|\delta|[A_{Lk}\,(\hat{d}_j + \hat{d}_{j'}\,\ln|\delta| + \hat{d}''_j\,\ln^2|\delta|) + A^-_{Sk}\,\tilde{b}_j + \bar{Z}''_{m_k+j} + \bar{Z}'''_{m_k+j}\,\ln|\delta|] + \mathcal{O}(\delta^2), \tag{191}$$

in the special case. In both cases, $j \neq 0$. The previous expressions are used to "jump" the solutions of the outer-region ODEs across the various rational surfaces in the plasma, while preventing them from approaching the surfaces too closely.

Consider a solution that is launched from the kth rational surface, so that $A_{Lk} = A^-_{Sk} = 0$. It follows from the preceding analysis that

$$\psi_{m_k}(r_k+|\delta|) = A^+_{Sk}\,|\delta|^{\nu_{S\,k}} + \mathcal{O}(\delta^2), \tag{192}$$

$$Z_{m_k}(r_k+|\delta|) = A^+_{Sk}\,b_S\,|\delta|^{\nu_{S\,k}} + \mathcal{O}(\delta^2), \tag{193}$$

$$\psi_{m_k+j}(r_k+|\delta|) = A^+_{Sk}\,\tilde{a}_j\,|\delta|^{\nu_{S\,k}} + \mathcal{O}(\delta^2), \tag{194}$$

$$Z_{m_k+j}(r_k+|\delta|) = A^+_{Sk}\,\tilde{b}_j\,|\delta|^{\nu_{S\,k}} + \mathcal{O}(\delta^2), \tag{195}$$

for $j \neq 0$. The previous expression is used to launch "small" solutions from the various rational surfaces in the plasma, while preventing them from approaching the launching surfaces too closely.

It is helpful to define the quantities[6]

$$\Psi_k = r_k^{\nu_{L\,k}}\left(\frac{\nu_{Sk}-\nu_{Lk}}{L^{m_k}_{m_k}}\right)^{1/2}_{r_k} A_{Lk}, \tag{196}$$

$$\Delta\Psi_k = r_k^{\nu_{S\,k}}\left(\frac{\nu_{Sk}-\nu_{Lk}}{L^{m_k}_{m_k}}\right)^{1/2}_{r_k} (A^+_{Sk} - A^-_{Sk}), \tag{197}$$

at each rational surface in the plasma. Here, the complex parameter Ψ_k is a measure of the reconnected helical magnetic flux at the kth rational surface, whereas the complex parameter $\Delta\Psi_k$ is a measure of the strength of a localized current sheet that flows parallel to the equilibrium magnetic field at the surface. It is evident from Eqs. (117), (119)–(121), (124), (125), (127), (129), (130), and (183)–(197) that[6,16]

$$T_\phi(r) = \int_0^r \sum_{k=1,K} \delta T_k\,\delta(\tilde{r}-r_k)\,d\tilde{r}, \tag{198}$$

where

$$\delta T_k = 2\pi^2\,n\,\mathrm{Im}(\Psi^*_k\,\Delta\Psi_k). \tag{199}$$

Here, δT_k is the net toroidal electromagnetic torque exerted on the plasma in the immediate vicinity of the kth rational surface.

VI. VACUUM SOLUTION

A. Plasma/vacuum interface

Let the plasma/vacuum interface correspond to $r = \epsilon$, where ϵ is the inverse aspect ratio of the plasma. In other words, let $\epsilon = a/R_0$, where a is the effective minor radius of the plasma. The region external to the plasma, $r > \epsilon$, is assumed to be free of non-axisymmetric currents.

B. Perturbed vacuum magnetic field

In the vacuum region $r > \epsilon$, the curl-free perturbed magnetic field can be written in the form[6]

$$\mathbf{b} = \mathrm{i}\,\nabla[V(r,\theta)\,\exp(-\mathrm{i}\,n\,\phi)]. \tag{200}$$

The physical constraint $\nabla\cdot\mathbf{b} = 0$ implies that

$$\nabla^2[V(r,\theta)\,\exp(-\mathrm{i}\,n\,\phi)] = 0. \tag{201}$$

C. Toroidal coordinates

It is necessary to obtain a solution of the previous equation that extends to infinity. This goal can be achieved using *orthogonal toroidal coordinates*, μ, η, and ϕ, where[32]

$$R = \frac{\sinh\mu}{\cosh\mu - \cos\eta}, \tag{202}$$

$$Z = \frac{\sin\eta}{\cosh\mu - \cos\eta}. \tag{203}$$

Here, $\mu(R,Z) \to 0$ corresponds to either $R \to 0$ or $(R^2+Z^2)^{1/2} \to \infty$ (i.e., an approach to the toroidal symmetry axis or to infinity), whereas $\mu(R,Z) \to \infty$ corresponds to $(R,Z) \to (1,0)$ (i.e., an approach to the magnetic axis). Furthermore, $\eta(R,Z)$ is an angular variable in the poloidal plane.

The most general solution of Eq. (201), in toroidal coordinates, that satisfies the physical constraint that the scalar magnetic potential, V, is well-behaved a long way from the plasma, can be written[33]

$$V(z,\eta) = a_0\,\frac{\sqrt{\pi}\,\Gamma(1/2-n)}{\sqrt{2}}\,(z-\cos\eta)^{1/2}\,P^n_{-1/2}(z) + \sum_{m\neq 0} a_m\,\cos(|m|\,\pi)\,\frac{\sqrt{\pi}\,\Gamma(|m|+1/2-n)\,\epsilon^{|m|}}{2^{|m|-1/2}\,|m|!} \times (z-\cos\eta)^{1/2}\,P^n_{m-1/2}(z)\,\exp(-\mathrm{i}\,m\,\eta), \tag{204}$$

where $z = \cosh\mu$, the $P^n_{m-1/2}(z)$ are *toroidal functions*,[34] $\Gamma(z)$ is a gamma function,[35] and the a_m are arbitrary complex coefficients. Here, the normalization of the a_m is the same as that adopted in Ref. 6.

D. Vacuum solution at plasma/vacuum interface

In the vicinity of the plasma/vacuum interface, we can write

$$V(r,\theta) = \sum_m V_m(r)\, \exp(\mathrm{i}\, m\,\theta), \tag{205}$$

where

$$V_m(\epsilon) = \oint_{r=\epsilon} V\, \exp(-\mathrm{i}\, m\,\theta)\, \frac{d\theta}{2\pi} = \sum_{m'} \mathcal{P}_m^{m'}\, a_{m'}, \tag{206}$$

and, according to Eq. (204),

$$\mathcal{P}_m^{m'} = \cos(|m'|\,\pi)\, \frac{\sqrt{\pi}\,\Gamma(|m'|+1/2-n)\,\epsilon^{|m'|}}{2^{|m'|-1/2}\,|m'|!} \oint_{r=\epsilon} (z-\cos\eta)^{1/2} \times P^n_{m'-1/2}(z)\, \exp\left[-\mathrm{i}\,(m\,\theta + m'\,\eta)\right] \frac{d\theta}{2\pi} \tag{207}$$

for general m', and

$$\mathcal{P}_m^0 = \frac{\sqrt{\pi}\,\Gamma(1/2-n)}{\sqrt{2}} \oint_{\hat{r}=1} (z-\cos\eta)^{1/2}\, P^n_{-1/2}(z)\, \exp(-\mathrm{i}\, m\,\theta)\, \frac{d\theta}{2\pi} \tag{208}$$

for the special case $m' = 0$.

Let

$$\mathcal{J}\,\mathbf{b}\cdot\nabla r = \mathrm{i}\,\psi(r,\theta)\, \exp(-\mathrm{i}\, n\,\phi). \tag{209}$$

In the vicinity of the plasma/vacuum interface, we can write

$$\psi(r,\theta) = \sum_m \psi_m(r)\, \exp(\mathrm{i}\, m\,\theta), \tag{210}$$

where

$$\psi_m(\epsilon) = \oint_{r=\epsilon} \mathcal{J}\,\nabla V\cdot\nabla r\, \exp(-\mathrm{i}\, m\,\theta)\, \frac{d\theta}{2\pi} = \sum_{m'} \mathcal{R}_m^{m'}\, a_{m'}, \tag{211}$$

and, according to Eq. (204),

$$\mathcal{R}_m^{m'} = \cos(|m'|\,\pi)\, \frac{\sqrt{\pi}\,\Gamma(|m'|+1/2-n)\,\epsilon^{|m'|}}{2^{|m'|-1/2}\,|m'|!} \times \oint_{r=\epsilon} \left\{ \left[\frac{1}{2}\,(z-\cos\eta)^{-1/2}\, P^n_{m'-1/2}(z) + (z-\cos\eta)^{1/2}\, \frac{dP^n_{m'-1/2}}{dz} \right] \mathcal{J}\,\nabla r\cdot\nabla z + \left[\frac{1}{2}\,(z-\cos\eta)^{-1/2}\, \sin\eta - \mathrm{i}\, m'\,(z-\cos\eta)^{1/2} \right] \times P^n_{m'-1/2}(z)\, \mathcal{J}\,\nabla r\cdot\nabla\eta \right\} \exp\left[-\mathrm{i}\,(m\,\theta + m'\,\eta)\right] \frac{d\theta}{2\pi}, \tag{212}$$

for general m', and

$$\mathcal{R}_m^0 = \frac{\sqrt{\pi}\,\Gamma(1/2-n)}{\sqrt{2}} \oint_{r=\epsilon} \left\{ \left[\frac{1}{2}\,(z-\cos\eta)^{-1/2}\, P^n_{-1/2}(z) + (z-\cos\eta)^{1/2}\, \frac{dP^n_{-1/2}}{dz} \right] \mathcal{J}\,\nabla r\cdot\nabla z + \frac{1}{2}\,(z-\cos\eta)^{-1/2} \times \sin\eta\, P^n_{-1/2}(z)\, \nabla r\cdot\nabla\eta \right\} \exp(-\mathrm{i}\, m\,\theta)\, \frac{d\theta}{2\pi}, \tag{213}$$

for the special case $m' = 0$.

E. Homogeneous boundary condition at plasma/vacuum interface

According to Eqs. (49), (78), (80), (99)–(101), (200), and (205),

$$V_m(r) = \frac{Z_m(r)}{m - n\,q(r)}, \tag{214}$$

and the $\psi_m(r)$ defined in Eq. (98) can be identified with the $\psi_m(r)$ defined in Eqs. (209) and (210). Thus, given that ψ and Z must be continuous across the plasma/vacuum interface (in the absence of finite edge equilibrium plasma currents), Eqs. (206) and (211) yield the following homogenous boundary condition at the interface:

$$\frac{Z_m(\epsilon)}{m - n\,q(\epsilon)} = \sum_{m'} H_{mm'}\, \psi_{m'}(\epsilon), \tag{215}$$

where

$$\sum_{m''} H_{mm''}\, \mathcal{R}_{m''}^{m'} = \mathcal{P}_m^{m'}. \tag{216}$$

F. Toroidal electromagnetic angular momentum flux

By analogy with Eq. (116), the outward flux of toroidal electromagnetic angular momentum across the plasma/vacuum interface, which is equal to the flux of toroidal electromagnetic angular momentum across a surface of constant μ (in the direction of decreasing μ) in the vacuum region, is given by

$$T_\phi(\epsilon) = -\oint\oint (\nabla\mu\times\nabla\eta\cdot\nabla\phi)^{-1}\, b_\phi\, b^\mu\, d\eta\, d\phi = -\frac{\mathrm{i}\,\pi\, n}{2} \oint \frac{z^2-1}{z-\cos\eta} \left(\frac{\partial V}{\partial z}\, V^* - \frac{\partial V^*}{\partial z}\, V \right) d\eta. \tag{217}$$

Making use of Eq. (204), we deduce that

$$T_\phi(\epsilon) = 0. \tag{218}$$

In other words, the flux of toroidal electromagnetic angular momentum across the vacuum/plasma interface is zero, as must be the case because an isolated tokamak plasma cannot exert a net toroidal electromagnetic torque on itself.[6]

According to Eq. (117), the outward flux of toroidal electromagnetic angular momentum across the plasma/vacuum interface can also be written as follows:

$$T_\phi(\epsilon) = \mathrm{i}\,\pi^2\, n \sum_m \left[\frac{Z_m^*\,\psi_m - \psi_m^*\, Z_m}{m - n\,q} \right]_{r=\epsilon}. \tag{219}$$

It follows from Eq. (215) that Eq. (218) can only be satisfied, in general, if the vacuum response matrix, $H_{mm'}$, is Hermitian.

G. Vacuum response matrix

It is clearly important to prove that the vacuum response matrix, $H_{mm'}$, is Hermitian. Otherwise, toroidal electromagnetic angular momentum is not conserved.

Let us assume that all perturbed quantities vary with the toroidal angle, ϕ, as $\exp(-\mathrm{i}\, n\, \phi)$. The vacuum region outside the plasma corresponds to the section, C (say), of the R, Z plane that lies between the curve $r = \epsilon$ and the curve $z = 1$. Let us define the function $\mathcal{E}_m(z, \mu)$ such that

$$\mathcal{E}_m = \exp(-\mathrm{i}\, m\, \theta) \quad \text{at } r = \epsilon, \tag{220}$$

$$\nabla^2 \mathcal{E}_m = \frac{n^2}{R^2}\, \mathcal{E}_m \quad \text{throughout } C, \tag{221}$$

$$\mathcal{E}_m = 0 \quad \text{at } z = 1. \tag{222}$$

In this section, ∇^2 denotes a two-dimensional Laplacian in the R, Z plane, and all vector analysis is two-dimensional, and takes place in the R-Z plane. Recall that

$$\nabla^2 V = \frac{n^2}{R^2}\, V \quad \text{throughout } C, \tag{223}$$

$$V = 0 \quad \text{at } z = 1. \tag{224}$$

It follows from Eq. (211) and (220) that

$$\psi_m(\epsilon) = \oint_{r=\epsilon} \mathcal{J}\, \mathcal{E}_m\, \nabla V \cdot \nabla r\, \frac{d\theta}{2\pi}. \tag{225}$$

The previous equation can also be written

$$\psi_m(\epsilon) = -\frac{1}{2\pi} \oint_S \mathcal{E}_m\, \nabla V \cdot d\mathbf{S}, \tag{226}$$

where S is the bounding surface of the vacuum domain, C, and use has been made of Eqs. (222) and (224). Note that $d\mathbf{S} = -\mathcal{J}\, \nabla r\, d\theta$. Now,

$$\oint_S (\mathcal{E}_m\, \nabla V - V\, \nabla \mathcal{E}_m) \cdot d\mathbf{S} = \int_C \nabla \cdot (\mathcal{E}_m\, \nabla V - V\, \nabla \mathcal{E}_m) dC = \int_C (\mathcal{E}_m\, \nabla^2 V - V\, \nabla^2 \mathcal{E}_m) dC = 0, \tag{227}$$

where use has been made of Eqs. (221) and (223). The previous three equations imply that

$$\psi_m(\epsilon) = -\frac{1}{2\pi} \oint_S V\, \nabla \mathcal{E}_m \cdot d\mathbf{S} = \oint_{r=\epsilon} \mathcal{J}\, V\, \nabla \mathcal{E}_m \cdot \nabla r\, \frac{d\theta}{2\pi}, \tag{228}$$

where use has been made of Eqs. (222) and (224). Thus, in accordance with Eqs. (206), (214), and (215), we can write

$$\psi_m(\epsilon) = \sum_{m'} H^{-1}_{mm'}\, V_{m'}(\epsilon), \tag{229}$$

where

$$H^{-1}_{mm'} = \oint_{r=\epsilon} \mathcal{J}\, \nabla \mathcal{E}_m \cdot \nabla r\, \exp(\mathrm{i}\, m'\, \theta)\, \frac{d\theta}{2\pi}. \tag{230}$$

The inverse vacuum response matrix can be written as follows:

$$H^{-1}_{mm'} = -\frac{1}{2\pi} \oint_S \mathcal{E}^*_{m'}\, \nabla \mathcal{E}_m \cdot d\mathbf{S}, \tag{231}$$

where use has been made of Eqs. (220), (222), and (230). It follows that

$$H^{-1}_{mm'} - H^{-1*}_{m'm} = -\frac{1}{2\pi} \oint_S (\mathcal{E}^*_{m'}\, \nabla \mathcal{E}_m - \mathcal{E}_m\, \nabla \mathcal{E}^*_{m'}) \cdot d\mathbf{S} - \frac{1}{2\pi} \int_C \nabla \cdot (\mathcal{E}^*_{m'}\, \nabla \mathcal{E}_m - \mathcal{E}_m\, \nabla \mathcal{E}^*_{m'}) dC - \frac{1}{2\pi} \int_C (\mathcal{E}^*_{m'}\, \nabla^2 \mathcal{E}_m - \mathcal{E}_m\, \nabla^2 \mathcal{E}^*_{m'}) dC = 0, \tag{232}$$

where use has been made of Eq. (221). Thus, we conclude that $H^{-1}_{mm'}$, as defined in Eq. (230), is Hermitian. It follows that the vacuum response matrix, $H_{mm'}$, is also Hermitian.

VII. INVERSE ASPECT-RATIO EXPANDED TOKAMAK EQUILIBRIUM

A. Equilibrium magnetic flux surfaces

Let us assume that the inverse aspect ratio of the plasma, ϵ, is such that $0 < \epsilon \ll 1$. Let $r = \epsilon\, \hat{r}$, $\nabla = \epsilon^{-1}\, \hat{\nabla}$, and $' \rightarrow \epsilon^{-1}\, '$. Suppose that the loci of the equilibrium magnetic flux surfaces can be written in the parametric form:[2,6,21,36]

$$R(\hat{r}, \omega) = 1 - \epsilon\, \hat{r}\, \cos\omega + \epsilon^2 \sum_{j>0} H_j(\hat{r})\, \cos[(j-1)\,\omega] + \epsilon^2 \sum_{j>1} V_j(\hat{r})\, \sin[(j-1)\,\omega] + \epsilon^3\, L(\hat{r})\, \cos\omega, \tag{233}$$

$$Z(\hat{r}, \omega) = \epsilon\, \hat{r}\, \sin\omega + \epsilon^2 \sum_{j>1} H_j(\hat{r})\, \sin[(j-1)\,\omega] - \epsilon^2 \sum_{j>1} V_j(\hat{r})\, \cos[(j-1)\,\omega] - \epsilon^3\, L(\hat{r})\, \sin\omega, \tag{234}$$

where j is a positive integer. Here, $H_1(\hat{r})$ controls the relative horizontal locations of the flux-surface centroids, $H_2(\hat{r})$ and $V_2(\hat{r})$ control the magnitudes and vertical tilts of the flux-surface ellipticities, $H_3(\hat{r})$ and $V_3(\hat{r})$ control the magnitudes and vertical tilts of the flux-surface triangularities, etc., whereas $L(\hat{r})$ is a flux-surface relabeling parameter. Moreover, $\omega(R, Z)$ is a poloidal angle that is distinct from θ. Note that V_1 does not appear in Eq. (234) because such a factor merely gives rise to a rigid vertical shift of the plasma that can be eliminated by a suitable choice of the origin of the flux-coordinate system.[36]

Let

$$J(\hat{r}, \omega) = \frac{1}{\epsilon^2} \left(\frac{\partial R}{\partial \omega} \frac{\partial Z}{\partial \hat{r}} - \frac{\partial R}{\partial \hat{r}} \frac{\partial Z}{\partial \omega} \right) \tag{235}$$

be the Jacobian of the $\hat{r}$, ω coordinate system. We can transform to the $\hat{r}$, θ coordinate system by writing

$$\theta(\hat{r}, \omega) = 2\pi \int_0^{\omega} \frac{J(\hat{r}, \tilde{\omega})}{R(\hat{r}, \tilde{\omega})}\, d\tilde{\omega} \Big/ \oint \frac{J(\hat{r}, \omega)}{R(\hat{r}, \omega)}\, d\omega, \tag{236}$$

$$\hat{r} = \frac{1}{2\pi} \oint \frac{J(\hat{r}, \omega)}{R(\hat{r}, \omega)}\, d\omega. \tag{237}$$

This transformation ensures that

$$\frac{\partial \theta}{\partial \omega} = \frac{J}{\hat{r}\, R}, \tag{238}$$

and, hence, that

$$\mathcal{J} \equiv \frac{R}{\epsilon}\left(\frac{\partial R}{\partial \theta}\frac{\partial Z}{\partial \hat{r}} - \frac{\partial R}{\partial \hat{r}}\frac{\partial Z}{\partial \theta}\right) = \epsilon\, R J \frac{\partial \omega}{\partial \theta} = r R^2, \tag{239}$$

in accordance with Eq. (2).

B. Metric elements

We can determine the metric elements of the flux-coordinate system by combining Eqs. (233)–(237). Evaluating the elements up to $\mathcal{O}(\epsilon)$, but retaining $\mathcal{O}(\epsilon^2)$ contributions to terms that are independent of ω, we obtain[6,21,36]

$$L(\hat{r}) = \frac{\hat{r}^3}{8} - \frac{\hat{r}\,H_1}{2} - \frac{1}{2}\sum_{j>1}(j-1)\,\frac{H_j^2}{\hat{r}} - \frac{1}{2}\sum_{j>1}(j-1)\,\frac{V_j^2}{\hat{r}}, \tag{240}$$

$$\theta = \omega + \epsilon\,\hat{r}\,\sin\omega - \epsilon\sum_{j>0}\frac{1}{j}\left[H_j' - (j-1)\,\frac{H_j}{\hat{r}}\right]\sin(j\,\omega) + \epsilon\sum_{j>1}\frac{1}{j}\left[V_j' - (j-1)\,\frac{V_j}{\hat{r}}\right]\cos(j\,\omega), \tag{241}$$

$$|\hat{\nabla}\hat{r}|^2 = 1 + 2\,\epsilon\sum_{j>0} H_j'\,\cos(j\,\theta) + 2\,\epsilon\sum_{j>1} V_j'\,\sin(j\,\theta) + \epsilon^2\left(\frac{3\,\hat{r}^2}{4} - H_1 + \frac{1}{2}\sum_{j>0}\left[H_j'^2 + (j^2-1)\,\frac{H_j^2}{\hat{r}^2}\right] + \frac{1}{2}\sum_{j>1}\left[V_j'^2 + (j^2-1)\,\frac{V_j^2}{\hat{r}^2}\right]\right), \tag{242}$$

$$\hat{\nabla}\hat{r}\cdot\hat{\nabla}\theta = \epsilon\,\sin\theta - \epsilon\sum_{j>0}\frac{1}{j}\left[H_j'' + \frac{H_j'}{\hat{r}} + (j^2-1)\,\frac{H_j}{\hat{r}^2}\right]\sin(j\theta) + \epsilon\sum_{j>1}\frac{1}{j}\left[V_j'' + \frac{V_j'}{\hat{r}} + (j^2-1)\,\frac{V_j}{\hat{r}^2}\right]\cos(j\theta), \tag{243}$$

$$R^2 = 1 - 2\,\epsilon\,\hat{r}\,\cos\theta - \epsilon^2\left(\frac{\hat{r}^2}{2} - \hat{r}\,H_1' - 2\,H_1\right). \tag{244}$$

Here, $' \equiv d/d\hat{r}$. Moreover, we have made use of the fact that $V_j \propto H_j$, for $j > 1$, because V_j and H_j satisfy the identical differential equations, (250) and (251).

C. Expansion of Grad–Shafranov equation

Let us write

$$f(\hat{r}) = \epsilon\,\frac{\hat{r}\,g}{q}, \tag{245}$$

$$g(\hat{r}) = 1 + \epsilon^2\,g_2(\hat{r}) + \epsilon^4\,g_4(\hat{r}), \tag{246}$$

$$P'(\hat{r}) = \epsilon^2\,p_2'(\hat{r}), \tag{247}$$

where q, g_2, g_4, and p_2 are all $\mathcal{O}(1)$. Here, the safety factor, $q(\hat{r})$, and the second-order plasma pressure gradient, $p_2'(\hat{r})$, are the two free flux-surface functions that characterize the plasma equilibrium.[25]

Expanding the Grad–Shafranov equation (16) order by order in the small parameter ϵ, making use of Eqs. (242)–(247), we obtain[2,4,21,36]

$$g_2' = -p_2' - \frac{\hat{r}}{q^2}\,(2-s), \tag{248}$$

$$H_1'' = -(3-2\,s)\,\frac{H_1'}{\hat{r}} - 1 + \frac{2\,p_2'\,q^2}{\hat{r}}, \tag{249}$$

$$H_j'' = -(3-2\,s)\,\frac{H_j'}{\hat{r}} + (j^2-1)\,\frac{H_j}{\hat{r}^2} \quad \text{for } j>1, \tag{250}$$

$$V_j'' = -(3-2\,s)\,\frac{V_j'}{\hat{r}} + (j^2-1)\,\frac{V_j}{\hat{r}^2} \quad \text{for } j>1, \tag{251}$$

$$g_4' = -\frac{\hat{r}}{q^2}\left(\frac{3\,\hat{r}^2}{2} - 2\,\hat{r}\,H_1' + \sum_{j>0}\left[H_j'^2 + 2\,(j^2-1)\,\frac{H_j'\,H_j}{\hat{r}} - (j^2-1)\,\frac{H_j^2}{\hat{r}^2}\right] + \sum_{j>1}\left[V_j'^2 + 2\,(j^2-1)\,\frac{V_j'\,V_j}{\hat{r}} - (j^2-1)\,\frac{V_j^2}{\hat{r}^2}\right]\right) + \frac{\hat{r}}{q^2}\,(2-s)\left(-g_2 - \frac{3\,\hat{r}^2}{4} + \frac{\hat{r}^2}{q^2} + H_1 + \frac{1}{2}\sum_{j>0}\left[3\,H_j'^2 - (j^2-1)\,\frac{H_j^2}{\hat{r}^2}\right] + \frac{1}{2}\sum_{j>1}\left[3\,V_j'^2 - (j^2-1)\,\frac{V_j^2}{\hat{r}^2}\right]\right) + p_2'\left(g_2 + \frac{\hat{r}^2}{2} + \frac{\hat{r}^2}{q^2} - 2\,H_1 - 3\,\hat{r}\,H_1'\right). \tag{252}$$

Note that the relative horizontal shift of magnetic flux surfaces, H_1, otherwise known as the *Shafranov shift*,[37] is driven by toroidicity [the second term on the right-hand side of Eq. (249)], and plasma pressure gradients (the third term). All of the other shaping terms (i.e., the H_j, for $j > 1$, and the V_j) are driven by axisymmetric currents flowing in external magnetic field coils.[36]

Finally, it follows from Eqs. (38), (39), (71), and (245)–(247) that

$$\alpha_p(\hat{r}) = \frac{p_2'\,q^2}{\hat{r}}\,(1 - 2\,\epsilon^2\,g_2), \tag{253}$$

$$\alpha_g(\hat{r}) = \frac{q}{\hat{r}}\,(g_2' - \epsilon^2\,g_2\,g_2' + \epsilon^2\,g_4'), \tag{254}$$

$$\alpha_f(\hat{r}) = -s + \epsilon^2\,\hat{r}\,g_2'. \tag{255}$$

D. Self-inductance and β values

The conventionally defined normalized self-inductance, toroidal beta, poloidal beta, and normalized beta values of the plasma equilibrium can be written as follows:[25]

$$l_i = \frac{2\int_0^1 \hat{r}\,f^2\,\langle|\nabla r|^2\rangle\,d\hat{r}}{\left(f^2\,\langle|\nabla r|^2\rangle^2\right)_{\hat{r}=1}}, \tag{256}$$

$$\beta_t = \frac{2\,\epsilon^2\int_0^1 \hat{r}\,\langle R^2\rangle\,p_2\,d\hat{r}}{\int_0^1 \hat{r}\,(1 + 2\,\epsilon^2\,g_2)\,d\hat{r}}, \tag{257}$$

$$\beta_p = \frac{2\,\epsilon^2\int_0^1 \hat{r}\,\langle R^2\rangle\,p_2\,d\hat{r}}{\int_0^1 \hat{r}\,f^2\,\langle|\nabla r|^2\rangle\,d\hat{r}}, \tag{258}$$

$$\beta_N = \frac{20\,\beta_t}{(f\,\langle|\nabla r|^2\rangle)_{\hat{r}=1}}, \tag{259}$$

respectively. Here, $\langle\cdots\rangle \equiv \oint(\cdots)\,d\theta/2\pi$.

E. Coupling coefficients

Let

$$S_1(\hat{r}) = \frac{1}{2}\sum_{j>0}\left[3\,(H_j'^2 + V_j'^2) - (j^2-1)\,\frac{H_j^2+V_j^2}{\hat{r}^2}\right], \tag{260}$$

$$S_2(\hat{r}) = \sum_{j>1} 2\,(j^2-1)\left(H_j'^2 + V_j'^2 - \frac{11}{3}\frac{H_j'H_j + V_j'V_j}{\hat{r}} + j^2\frac{H_j^2+V_j^2}{\hat{r}^2}\right) - \sum_{j>0}(1-s)\left(\frac{H_j'H_j + V_j'V_j}{\hat{r}} + \frac{1}{3}\frac{H_j^2+V_j^2}{\hat{r}^2}\right). \tag{261}$$

The analysis of Secs. IV A, IV B, VII B, and VII C can be combined to give the following expressions for the coupling coefficients appearing in the outer-region o.d.e.s, (102) and (103):[6]

$$L_m^m(\hat{r}) = m^2 + \epsilon^2 m^2\left(-\frac{3\,\hat{r}^2}{4} + H_1 + S_1\right) + \epsilon^2 n^2\,\hat{r}^2, \tag{262}$$

$$M_m^m(\hat{r}) = 0, \tag{263}$$

$$N_m^m(\hat{r}) = 0, \tag{264}$$

$$P_m^m(\hat{r}) = (m-nq)^2 + \frac{m-nq}{m}\,q\hat{r}\,\frac{d}{d\hat{r}}\left(\frac{2-s}{q}\right) + \epsilon^2(m-nq)^2\left\{\frac{7\hat{r}^2}{4} - H_1 - 3\hat{r}\,H_1' + S_1 + \frac{1}{m^2}\left[\frac{n}{m}\hat{r}\,\frac{d}{d\hat{r}}\left(\hat{r}^2\frac{2-s}{q}\right) - \hat{r}^2\frac{(2-s)^2}{q^2} - \hat{r}\,\frac{d}{d\hat{r}}(\hat{r}\,p_2')\right]\right\} - \epsilon^2\frac{m-nq}{m}\left\{2\hat{r}\,p_2'(2-s) + q\hat{r}\,\frac{d}{d\hat{r}} \times \left[\hat{r}^2\frac{2-s}{q^3} + \frac{s}{q}\left(\frac{3\hat{r}^2}{4} - H_1 - S_1\right) - \frac{2}{q}\left(\frac{3\hat{r}^2}{2} - H_1 - \hat{r}\,H_1' - \frac{2}{3}S_1\right)\right] - S_2\right\} + \epsilon^2\,2\hat{r}\,p_2'(1-q^2), \tag{265}$$

$$L_m^{m\pm1}(\hat{r}) = -\epsilon\,m\,(m\pm1)\,H_1', \tag{266}$$

$$L_m^{m\pm j}(\hat{r}) = -\epsilon\,m\,(m\pm j)\,(H_j' \pm \mathrm{i}\,V_j') \quad \text{for } j>1, \tag{267}$$

$$M_m^{m\pm1}(\hat{r}) = \mp\epsilon\,m\,(m-nq)\,p_2'\,q^2 \pm \epsilon\,m\,(m\pm1-nq) \times \left[\hat{r} + (1-s)\,H_1'\right], \tag{268}$$

$$M_m^{m\pm j}(\hat{r}) = \pm\epsilon\,\frac{m}{j}\,(m\pm j-nq) \times \left[(1-s)\,(H_j' \pm \mathrm{i}\,V_j') - (j^2-1)\,\frac{H_j \pm \mathrm{i}\,V_j}{\hat{r}}\right] \quad \text{for } j>1, \tag{269}$$

$$N_m^{m\pm1}(\hat{r}) = \mp\epsilon\,(m\pm1)\,(m\pm1-nq)\,p_2'\,q^2 \pm \epsilon\,(m\pm1) \times (m-nq)\left[\hat{r} + (1-s)\,H_1'\right], \tag{270}$$

$$N_m^{m\pm j}(\hat{r}) = \pm\epsilon\,\frac{(m\pm j)}{j}\,(m-nq) \times \left[(1-s)\,(H_j' \pm \mathrm{i}\,V_j') - (j^2-1)\,\frac{H_j \pm \mathrm{i}\,V_j}{\hat{r}}\right] \quad \text{for } j>1, \tag{271}$$

$$P_m^{m\pm1}(\hat{r}) = -\epsilon\,(1+s)\,p_2'\,q^2 + \epsilon\,(m-nq)\,(m\pm1-nq)\,(\hat{r} - H_1'), \tag{272}$$

$$P_m^{m\pm j}(\hat{r}) = -\epsilon\,(m-nq)\,(m\pm j-nq)\,(H_j' \pm \mathrm{i}\,V_j')] \text{ for } j>1. \tag{273}$$

When $m=0$, some of the coupling coefficient take on special values

$$P_0^0(\hat{r}) = n^2\,q^2 - \frac{q^2}{\hat{r}}\,\frac{d}{d\hat{r}}\left(\hat{r}^2\,\frac{2-s}{q^2}\right) - q^2\,\hat{r}\,\frac{d}{d\hat{r}}\left(\frac{p_2'}{\hat{r}}\right), \tag{274}$$

$$M_{\pm1}^0(\hat{r}) = \lim_{m\to0} M_{m\pm1}^m \mp\epsilon\,(2-s)\,H_1', \tag{275}$$

$$M_{\pm j}^0(\hat{r}) = \lim_{m\to0} M_{m\pm j}^m \mp \epsilon\,(2-s)\,j\,(H_j' \mp \mathrm{i}\,V_j') \quad \text{for } j>1, \tag{276}$$

$$N_0^{\pm1}(\hat{r}) = \lim_{m\to0} N_m^{m\pm1} \pm \epsilon\,(2-s)\,H_1', \tag{277}$$

$$N_0^{\pm j}(\hat{r}) = \lim_{m\to0} N_m^{m\pm j} \pm \epsilon\,(2-s)\,j\,(H_j' \pm \mathrm{i}\,V_j') \quad \text{for } j>1, \tag{278}$$

$$P_{\pm1}^0(\hat{r}) = \lim_{m\to0} P_{m\pm1}^m - \epsilon(2-s)\{\pm nq^3\,p_2' + (1\mp nq)[\hat{r} + (1-s)\,H_1']\}, \tag{279}$$

$$P_{\pm j}^0(\hat{r}) = \lim_{m\to0} P_{m\pm j}^m - \epsilon\,(2-s)\,\frac{(j\mp nq)}{j} \times \left[(1-s)\,(H_j' \mp \mathrm{i}\,V_j') - (j^2-1)\left(\frac{H_j \mp \mathrm{i}\,V_j}{\hat{r}}\right)\right] \text{ for } j>1, \tag{280}$$

$$P_0^{\pm1}(\hat{r}) = \lim_{m\to0} P_{m\pm1}^m - \epsilon(2-s)\{\pm nq^3\,p_2' + (1\mp nq)[\hat{r} + (1-s)\,H_1']\}, \tag{281}$$

$$P_0^{\pm j}(\hat{r}) = \lim_{m\to0} P_m^{m\pm j} - \epsilon\,(2-s)\,\frac{(j\mp nq)}{j} \times \left[(1-s)\,(H_j' \pm \mathrm{i}\,V_j') - (j^2-1)\left(\frac{H_j \pm \mathrm{i}\,V_j}{\hat{r}}\right)\right] \text{ for } j>1. \tag{282}$$

Here, the coupling coefficients are evaluated to $\mathcal{O}(\epsilon)$, while retaining $\mathcal{O}(\epsilon^2)$ contributions to diagonal terms.[4,6] Note that the coupling coefficients exactly satisfy the symmetry requirements (110)–(113).

F. Behavior close to magnetic axis

In the limit $\hat{r} \ll 1$, a well-behaved solution of the outer-region o.d.e.s, (102) and (103), with a dominant poloidal mode number $m>0$ is such that[6]

$$Z_m(\hat{r}) \simeq \frac{m-nq}{m}\,\psi_m(\hat{r}), \tag{283}$$

$$\psi_{m+1}(\hat{r}) \simeq -\epsilon\,\frac{\hat{r}[(m-nq) - 2\,p_2''\,q^2]}{2\,(m-nq)}\,\psi_m(\hat{r}), \tag{284}$$

$$\psi_{m+j}(\hat{r}) \simeq \epsilon \frac{2\,\hat{r}^2\,q''\,(H_j' - \mathrm{i}\,V_j')}{(m - n\,q)\,(m+1)\,q}\,\psi_m(\hat{r}) \quad \text{for } j > 1, \tag{285}$$

to lowest order, with all of the other Z_m and ψ_m approximately zero. A well-behaved solution with a dominant poloidal mode number $m < 0$ is such that

$$Z_m(\hat{r}) \simeq \frac{m - n\,q}{|m|}\,\psi_m(\hat{r}), \tag{286}$$

$$\psi_{m-1}(\hat{r}) \simeq -\epsilon \frac{\hat{r}\,[(m - n\,q) + 2\,p_2''\,q^2]}{2\,(m - n\,q)}\,\psi_m(\hat{r}), \tag{287}$$

$$\psi_{m-j}(\hat{r}) \simeq -\epsilon \frac{2\,\hat{r}^2\,q''\,(H_j' + \mathrm{i}\,V_j')}{(m - n\,q)\,(|m|+1)\,q}\,\psi_m(\hat{r}) \text{ for } j > 1, \tag{288}$$

to lowest order, with all of the other Z_m and ψ_m approximately zero. For the special case in which the dominant poloidal mode number is zero, the well-behaved solution is

$$Z_0(\hat{r}) \simeq \text{constant} \tag{289}$$

to lowest order, with all of the other Z_m and ψ_m approximately zero.

Note that the solutions (283)–(288) only exhibit "outward" coupling of different poloidal harmonics (i.e., coupling in the direction away from the $m = 0$ harmonic). However, the solutions whose central poloidal mode numbers are $m = \pm 1$ are special cases, and also exhibit inward coupling. Thus, in addition, to the couplings described in Eqs. (283)–(285), an $m = 1$ solution drives the harmonics

$$\psi_{1-j}(\hat{r}) \simeq 2\,\epsilon\,(H_j' - \mathrm{i}\,V_j')\,\psi_1(\hat{r}) \quad \text{for } j > 1. \tag{290}$$

Likewise, in addition to the couplings described in Eqs. (286)–(288), an $m = -1$ solution drives the harmonics

$$\psi_{-1+j}(\hat{r}) \simeq 2\,\epsilon\,(H_j' + \mathrm{i}\,V_j')\,\psi_{-1}(\hat{r}) \quad \text{for } j > 1. \tag{291}$$

G. Plasma/vacuum interface

We require the equilibrium plasma current to be zero at the plasma/vacuum interface, $\hat{r} = 1$, which implies that $g'(1) = P'(1) = 0$ (see Sec. II B). It follows from Eqs. (246)–(248) and (252) that we need[6]

$$p_2'(1) = 0, \tag{292}$$

$$s(1) = 2 + \epsilon^2 \left(\frac{3\,\hat{r}^2}{2} - 2\,\hat{r}\,H_1' + \sum_{j>0} \left[H_j'^2 + 2\,(j^2-1)\,\frac{H_j'\,H_j}{\hat{r}} - (j^2-1)\,\frac{H_j^2}{\hat{r}^2} \right] + \sum_{j>1} \left[V_j'^2 + 2\,(j^2-1)\,\frac{V_j'\,V_j}{\hat{r}} - (j^2-1)\,\frac{V_j^2}{\hat{r}^2} \right] \right)_{\hat{r}=1} + \mathcal{O}(\epsilon^4). \tag{293}$$

VIII. CALCULATION OF TEARING MODE DISPERSION RELATION

A. Introduction

Let the m_j, for $j = 0, J$, be the poloidal mode numbers included in the calculation. Here, it is assumed that $m_{j+1} = m_j + 1$ for $j = 0, J-1$. Let there be K rational surfaces in the plasma, and let the kth surface lie at radius $\hat{r}_k$, for $k = 1, K$. Here, it is assumed that $\hat{r}_{k+1} > \hat{r}_k$ for $k = 1, K-1$.

B. Well-behaved solutions launched from magnetic axis

Let us launch $J+1$ linearly independent, well-behaved solutions of the outer-region o.d.e.s, (102) and (103), from the magnetic axis, as described in Sec. VII F. Let us then numerically integrate these solutions to the plasma/vacuum interface. The poloidal harmonics of the solutions are denoted $\psi^a_{m_{j'}m_j}(\hat{r})$ and $Z^a_{m_{j'}m_j}(\hat{r})$, for $j, j' = 0, J$. Here, $m_{j'}$ is the poloidal mode number of the harmonic, whereas m_j is the dominant poloidal mode number of the solution close to the magnetic axis. The asymptotic matching conditions imposed at the rational surfaces are

$$A_{Lk}^- = A_{Lk}^+, \tag{294}$$

$$\Delta\Psi_k = 0, \tag{295}$$

for $k = 1, K$. [Eqs. (184)–(191) specify how these matching conditions are implemented at a given rational surface.] Let Π^a_{kj}, for $k = 1, K$ and $j = 0, J$, be the value of Ψ_k at the kth rational surface associated with a solution launched from the magnetic axis with dominant poloidal mode number m_j.

A scheme similar to A.H. Glasser's "fixups"[13] is employed to periodically re-orthogonalize the set of solutions. These re-orthogonalizations are implemented at user-defined locations between the magnetic axis and the plasma/vacuum interface. At each re-orthogonalization location, the matrix of solutions is forced to become upper triangular, via a process similar to Gaussian elimination, such that only one solution has a non-zero amount of the highest poloidal harmonic, two solutions have non-zero amounts of the next highest harmonic, and so on. The solutions are then renormalized to their largest component. The re-orthogonalizations are necessary to prevent the solutions from becoming colinear as a result of rounding errors, given the significantly different rates at which poloidal harmonics with different poloidal mode numbers grow with increasing $\hat{r}$ close to the magnetic axis. (In fact, a harmonic with mode number m grows as $\hat{r}^{|m|}$. Hence, an $m = 10$ harmonic grows far faster than an $m = 1$ harmonic. Unchecked, each solution would quickly become dominated by its component with the largest mode number.)

C. Small solutions launched from rational surfaces

Let us launch a "small" solution of the outer-region o.d.e.s from each rational surface in the plasma, as described in Secs. V B and V C, and numerically integrate it to the plasma/vacuum interface. The poloidal harmonics of the solutions are denoted $\psi^s_{m_jk}(\hat{r})$ and $Z^s_{m_jk}(\hat{r})$, for $j = 0, J$ and $k = 1, K$. Here, m_j is the poloidal mode number of the harmonic, whereas k is the index of the rational surface from which the solution is launched. The launch conditions are

$$A_{Lk}^- = A_{Lk}^+ = A_{Sk}^- = 0, \tag{296}$$

$$\Delta\Psi_k = 1. \tag{297}$$

[These launch conditions can be implemented at a given rational surface using Eqs. (192)–(195).] The asymptotic matching conditions imposed at the other rational surfaces are

$$A^{-}_{Lk'} = A^{+}_{Lk'}, \tag{298}$$

$$\Delta\Psi_{k'} = 0, \tag{299}$$

for $k' = k+1, K$. [Eqs. (184)–(191) again specify how these matching conditions are implemented at a given rational surface.] Let $\Pi^{s}_{k'k}$, for $k' = 1, K$ and $k = 1, K$, be the value of $\Psi_{k'}$ at the k' th rational surface associated with a small solution launched from the kth rational surface. Note that $\Pi^{s}_{k'k} = 0$ for $k' \leq k$.

D. Homogeneous toroidal tearing mode dispersion relation

The most general expression for the solution of the outer-region o.d.e.s at the plasma/vacuum interface is

$$\psi_{m_j}(1) = \sum_{j'=0,J} \psi^{a}_{m_j m_{j'}}(1)\,\alpha_{j'} + \sum_{k=1,K} \psi^{s}_{m_j k}(1)\,\Delta\Psi_k, \tag{300}$$

$$Z_{m_j}(1) = \sum_{j'=0,J} Z^{a}_{m_j m_{j'}}(1)\,\alpha_{j'} + \sum_{k=1,K} Z^{s}_{m_j k}(1)\,\Delta\Psi_k, \tag{301}$$

for $j = 0, J$, where the α_j are complex coefficients. However, the solution must satisfy the homogeneous boundary condition (215). It follows that

$$\sum_{j'=0,J} X_{jj'}\,\alpha_{j'} = \sum_{k=1,K} Y_{jk}\,\Delta\Psi_k \tag{302}$$

for $j = 0, J$, where

$$X_{jj'} = \frac{Z^{a}_{m_j m_{j'}}(1)}{m_j - n\,q(1)} - \sum_{j''=0,J} H_{m_j m_{j''}}\,\psi^{a}_{m_{j''} m_{j'}}(1), \tag{303}$$

$$Y_{jk} = \sum_{j'=0,J} H_{m_j m_{j'}}\,\psi^{s}_{m_{j'} k}(1) - \frac{Z^{s}_{m_j k}(1)}{m_j - n\,q(1)}, \tag{304}$$

for $j, j' = 0, J$ and $k = 1, K$. Thus, we can write

$$\alpha_j = \sum_{k=1,K} \Omega_{jk}\,\Delta\Psi_k \tag{305}$$

for $j = 0, J$, where

$$\sum_{j'=0,J} X_{jj'}\,\Omega_{j'k} = Y_{jk} \tag{306}$$

for $j = 0, J$ and $k = 1, K$. Our general solution is now free of arbitrary coefficients. Finally, making use of the definitions of the Π^{a}_{kj} and the $\Pi^{s}_{kk'}$ given in Secs. VIII B and VIII C, we obtain the *homogenous toroidal tearing mode dispersion relation*[3–6]

$$\Psi_k = \sum_{k'=1,K} F_{kk'}\,\Delta\Psi_{k'}, \tag{307}$$

for $k, k' = 1, K$, where

$$F_{kk'} = \sum_{j=0,J} \Pi^{a}_{kj}\,\Omega_{jk'} + \Pi^{s}_{kk'}. \tag{308}$$

Equation (307) specifies the reconnected helical magnetic flux, Ψ_k, driven at each rational surface in the plasma as a consequence of the current sheets, $\Delta\Psi_k$, flowing at the surfaces. It is clear that $F_{kk'}$ is a dimensionless inductance matrix.[38]

We can construct the "fully reconnected" tearing eigenfunction[6] associated with the kth rational surface, which is defined to have the following properties:

$$\Psi_{k'} = F_{k'k}, \tag{309}$$

$$\Delta\Psi_{k'} = \delta_{k'k}, \tag{310}$$

for $k' = 1, K$, as follows:

$$\psi^{f}_{m_j k}(\hat{r}) = \psi^{s}_{m_j k}(\hat{r}) + \sum_{j'=0,J} \psi^{a}_{m_j m_{j'}}(\hat{r})\,\Omega_{j'k}, \tag{311}$$

$$Z^{f}_{m_j k}(\hat{r}) = Z^{s}_{m_j k}(\hat{r}) + \sum_{j'=0,J} Z^{a}_{m_j m_{j'}}(\hat{r})\,\Omega_{j'k}, \tag{312}$$

for $j = 0, J$. Here, $\delta_{kk'}$ is a unit matrix. Note that the fully reconnected solution associated with the kth rational surface only has a current sheet at that surface. (The current sheets at the other surfaces are all zero.)

The homogeneous toroidal tearing mode dispersion relation can be written in the alternative form[3,6]

$$\Delta\Psi_k = \sum_{k'=1,K} E_{kk'}\,\Psi_{k'}, \tag{313}$$

for $k = 1, K$, where $E_{kk'}$ is the inverse of $F_{kk'}$. The previous equation specifies the current sheets driven at each rational surface in the plasma as a consequence of the reconnected fluxes at the surfaces.

We can construct the "unreconnected" tearing eigenfunction[6] associated with the kth rational surface, which is defined to have the following properties:

$$\Psi_{k'} = \delta_{k'k}, \tag{314}$$

$$\Delta\Psi_{k'} = E_{k'k}, \tag{315}$$

for $k' = 1, K$, as follows:

$$\psi^{u}_{m_j k}(\hat{r}) = \sum_{k'=1,K} \psi^{f}_{m_j k'}(\hat{r})\,E_{k'k}, \tag{316}$$

$$Z^{u}_{m_j k}(\hat{r}) = \sum_{k'=1,K} Z^{f}_{m_j k'}(\hat{r})\,E_{k'k}, \tag{317}$$

for $j = 0, J$. Note that the unreconnected solution associated with the kth rational surface only has reconnected flux at that surface. (The reconnected fluxes at the other surfaces are all zero.)

Let

$$\Delta_k = \frac{\Delta\Psi_k}{\Psi_k} \tag{318}$$

be the complex quantity that characterizes the tearing response of the resonant layer at the kth rational surface to the ideal-MHD solution in the outer region.[1] In general, Δ_k is a function of the growth-rate and phase-velocity of the reconnected helical magnetic flux at the surface.[6,39,40] Equations (313) and (318) can be combined to give the ultimate form of the tearing mode dispersion relation

$$\sum_{k'=1,k} (\Delta_k\,\delta_{kk'} - E_{kk'})\,\Psi_{k'} = 0, \tag{319}$$

for $k = 1, K$. It is clear that E_{kk} is the tearing stability index[1] at the kth rational surface when magnetic reconnection takes place at this surface, but is suppressed at the other surfaces (as is likely to be the case in the presence of sheared plasma rotation[6]).

E. Toroidal electromagnetic torques

According to Eqs. (199) and (313), the net toroidal electromagnetic torque exerted on an isolated plasma in the immediate vicinity of the kth rational surface is

$$\delta T_k = 2\pi^2\, n \sum_{k'=1,K} \mathrm{Im}(\Psi_k^*\, E_{kk'}\, \Psi_{k'}). \tag{320}$$

The total electromagnetic torque exerted on the plasma is

$$T_\phi(1) = \sum_{k=1,K} \delta T_k = 2\pi^2\, n \sum_{k,k'=1,K} \mathrm{Im}(\Psi_k^*\, E_{kk'}\, \Psi_{k'}). \tag{321}$$

However, we have already established that this total torque is zero, irrespective of the values of the Ψ_k [see Eq. (218)]. Thus, it follows that

$$E_{kk'} = E_{k'k}^*. \tag{322}$$

In other words, as a consequence of the conservation of toroidal electromagnetic angular momentum, the matrix $E_{kk'}$ must be Hermitian,[6] which implies that $F_{kk'}$ is also Hermitian (as ought to be the case if $F_{kk'}$ can be interpreted as a dimensionless inductance matrix).

IX. RESONANT MAGNETIC PERTURBATION COILS

A. Introduction

Suppose that the plasma is subject to a static, non-axisymmetric, resonant magnetic perturbation (RMP), with n periods in the toroidal direction, that is generated by currents flowing in magnetic field coils external to the plasma. Let us, rather simplistically, model these RMP coils as a set of L toroidal strands of negligible cross section in the R, Z plane. Suppose that the lth strand is located at $R = R_l$, $Z = Z_l$, and carries a net current $I_l \exp(-\mathrm{i}\, n\, \phi)$. Here, the complex quantity I_l specifies the amplitude and phase of the non-axisymmetric current flowing in the strand.

B. Externally generated perturbed magnetic field

Reusing the analysis of Sec. A of Ref. 41, the non-axisymmetric magnetic field generated by the currents flowing in the external magnetic field coils can be written $\mathbf{b}^x(R,\phi,Z) = \mathbf{b}^x(R,Z)\exp(-\mathrm{i}\, n\, \phi)$, where

$$\mathbf{b}^x(R,Z) = \nabla(R\, A_\phi) \times \nabla\phi, \tag{323}$$

$$A_\phi(R,Z) = \sum_{l=1,L} I_l\, G(R,Z;R_l,Z_l), \tag{324}$$

$$G(R,Z;R',Z') = \frac{(-1)^{n+1}\sqrt{\pi}\, R\, R'}{4\,\Gamma(n+1/2)} \left[\frac{\cosh\eta}{R^2+R'^2+(Z-Z')^2}\right]^{1/2} \times \left[(n-1/2)\, P_{-1/2}^{n-1}(\cosh\eta) + \frac{P_{-1/2}^{n+1}(\cosh\eta)}{n+1/2}\right], \tag{325}$$

$$\tanh\eta = \frac{2\, R\, R'}{R^2+R'^2+(Z-Z')^2}. \tag{326}$$

Here, the $P_{-1/2}^n(z)$ are toroidal functions.[34]

C. Inhomogeneous boundary condition at plasma/vacuum interface

According to Eqs. (2), (46), (78), (80), and (99)–(101), the magnetic perturbation at the plasma/vacuum interface generated by the currents flowing in the RMP coils is characterized by

$$\psi_m^x(1) = -\mathrm{i}\oint_{\hat{r}=1} \mathcal{J}\, \mathbf{b}^x \cdot \nabla r\, \exp(-\mathrm{i}\, m\, \theta)\, \frac{d\theta}{2\pi}, \tag{327}$$

$$\frac{Z_m^x(1)}{m - n\, q(1)} = n^{-1}\oint_{\hat{r}=1} R^2\, \mathbf{b}^x \cdot \nabla\phi\, \exp(-\mathrm{i}\, m\, \theta)\, \frac{d\theta}{2\pi}. \tag{328}$$

It follows from Eqs. (2) and (323) that

$$\psi_m^x(1) = m\oint_{\hat{r}=1} R\, A_\phi\, \exp(-\mathrm{i}\, m\, \theta)\, \frac{d\theta}{2\pi}, \tag{329}$$

$$\frac{Z_m^x(1)}{m - n\, q(1)} = 0, \tag{330}$$

where we have integrated by parts.

In the presence of the perturbed magnetic field generated by the RMP coils, the homogenous boundary condition at the plasma/vacuum interface (215) is modified to give the following inhomogeneous boundary condition:

$$\frac{Z_m(1)}{m - n\, q(1)} = \sum_{m'} H_{mm'} \left[\psi_{m'}(1) - \psi_{m'}^x(1)\right]. \tag{331}$$

D. Inhomogeneous toroidal tearing mode dispersion relation

The previous boundary condition can be combined with the analysis of Sec. VIII D to produce the following inhomogeneous toroidal tearing mode dispersion relation:[16,41]

$$\Delta\Psi_k = \sum_{k'=1,K} E_{kk'}\, \Psi_{k'} + \chi_k, \tag{332}$$

for $k = 1, K$, where

$$\chi_k = \sum_{k'=1,K} E_{kk'}\, \Lambda_{k'}, \tag{333}$$

$$\Lambda_k = \sum_{j=0,J} \Pi_{kj}^a\, \Upsilon_j, \tag{334}$$

$$\sum_{j'=0,J} X_{jj'}\, \Upsilon_{j'} = \Xi_j, \tag{335}$$

$$\Xi_j = \sum_{j'=0,J} H_{m_j m_{j'}}\, \psi_{m_{j'}}^x(1), \tag{336}$$

for $k = 1, K$ and $j = 0, J$.

The general tearing eigenfunction in the presence of the RMP can be written as

$$\psi_{m_j}(\hat{r}) = \sum_{k=1,K} \psi^u_{m_j k}(\hat{r})\, \Psi_k + \psi^{rmp}_{m_j}(\hat{r}), \tag{337}$$

$$Z_{m_j}(\hat{r}) = \sum_{k=1,K} Z^u_{m_j k}(\hat{r})\, \Psi_k + Z^{rmp}_{m_j}(\hat{r}), \tag{338}$$

for $j = 0, J$, where

$$\psi^{rmp}_{m_j}(\hat{r}) = \sum_{j'=0,J} \left[\sum_{k=1,K} \psi^u_{m_j k}(\hat{r}) - \psi^a_{m_j m_{j'}}(\hat{r}) \right] \Upsilon_{j'}, \tag{339}$$

$$Z^{rmp}_{m_j}(\hat{r}) = \sum_{j'=0,J} \left[\sum_{k=1,K} Z^u_{m_j k}(\hat{r}) - Z^a_{m_j m_{j'}}(\hat{r}) \right] \Upsilon_{j'}, \tag{340}$$

for $j = 0, J$. Here, $\psi^{rmp}_{m_j}(\hat{r})$ and $Z^{rmp}_{m_j}(\hat{r})$ represent the ideal MHD response of the plasma (i.e., the response in the absence of driven magnetic reconnection at the various rational surfaces in the plasma) to the currents flowing in the RMP coils.

E. Toroidal electromagnetic torques

Making use of Eqs. (199), (318), and (332), the toroidal electromagnetic torque exerted by the RMP coils at the kth rational surface in the plasma is

$$\delta T_k = 2\pi^2\, n\, \mathrm{Im}(\Delta_k)\, |\Psi_k|^2, \tag{341}$$

where

$$\sum_{k'=1,K} (\Delta_k\, \delta_{kk'} - E_{kk'})\, \Psi_{k'} = \chi_k, \tag{342}$$

for $k = 1, K$. In situations in which driven magnetic reconnection at the various rational surface in the plasma is strongly shielded by plasma rotation,[16,28] so that $|\Delta_k| \gg |E_{kk'}|$, for all k, k', Eq. (341) simplifies to give

$$\delta T_k \simeq 2\pi^2\, n\, \frac{\mathrm{Im}(\Delta_k)}{|\Delta_k|^2}\, |\chi_k|^2. \tag{343}$$

X. TJ CODE

A. Introduction

The first computer code that was developed in order to calculate the tearing mode stability of an aspect-ratio expanded tokamak plasma equilibrium was the T3 code (1998). The T3 code solves a set of coupled first-order o.d.e.s associated with the resonant poloidal harmonics at the various rational surfaces in the plasma, together with their upper and lower sidebands driven by toroidal coupling.[4] The T3 code was quickly followed by the T7 code (1993), which extends the calculation to describe the coupling of poloidal harmonics associated with the elliptic and triangular shaping of up-down-symmetric equilibrium magnetic flux-surfaces, necessitating seven coupled poloidal harmonics for each rational surface in the plasma.[6]

Unfortunately, both the T3 and T7 codes were formulated incorrectly, causing them to only conserve toroidal electromagnetic angular momentum at unrealistically low values of the inverse aspect ratio. The origin of the problem is apparent from the following equation, which can be derived from Eqs. (102), (103), and (117):

$$\frac{dT_\phi}{dr} = \mathrm{i}\,\pi^2\, n \sum_{m,m'=m_1,m_2} \left[\frac{(P^m_{m'} - P^{m'*}_m)\, \psi^*_m \psi_{m'} + (M^m_{m'} + N^{m'*}_m)\, \psi_m Z^*_{m'}}{(m - n\,q)\,(m' - n\,q)} \right. \tag{344}$$

$$\left. - \frac{(N^m_{m'} + M^{m'*}_m)\, Z_m \psi^*_{m'} - (L^m_{m'} - L^{m'*}_m)\, Z_m Z^*_{m'}}{(m - n\,q)\,(m' - n\,q)} \right]. \tag{345}$$

Here, we have truncated the number of poloidal harmonics included in the calculation such that only harmonics whose mode numbers lie in the range m_1–m_2 are included. Of course, such a truncation is a practical necessity. However, despite the truncation, toroidal angular momentum is conserved (i.e., $dT_\phi/dr = 0$ between rational surfaces) because of the symmetry properties of the coupling matrices, (110)–(113). In fact, in order to conserve angular momentum, it is necessary to include *all* couplings between poloidal harmonics whose mode numbers lie in a certain range, but to neglect *any* stray couplings to harmonics whose mode numbers lie outside this range. However, the T3/T7 code solutions are constructed from unbreakable triplets/sextuplets of coupled harmonics, whose mode numbers are grouped around a some central mode number. Moreover, the T3/T7 truncation scheme limits the number of triplets/sextuplets included in the calculation to those whose central mode numbers lie in a certain range. However, such a truncation scheme inevitably include stray couplings to poloidal harmonics whose mode numbers lie outside this range.

The recently developed TJ code (2024), which is an implementation of the analysis of Secs. II–IX of this paper, calculates the tearing stability of an aspect-ratio expanded tokamak equilibrium with magnetic flux surfaces of arbitrary shape. Moreover, the code has been formulated in such a fashion that it conserves toroidal electromagnetic angular momentum at realistic values of the inverse aspect ratio (because it includes all couplings between poloidal harmonics whose mode numbers lie in a given range and neglects couplings to harmonics whose mode numbers lie outside this range). As will become clear in the following discussion, conservation of angular momentum is a vitally important property of a toroidal tearing mode code.

B. Example plasma equilibrium

Let us investigate the stability of an example tokamak equilibrium to $n = 1$ tearing modes.

The example equilibrium is characterized by $\epsilon = 0.2$, $H_2(1) = 1.0$, $V_2(1) = 0.2$, $H_3(1) = 0.5$, $V_3(1) = -0.375$, and $H_j(1) = V_j(1) = 0$ for all $j > 3$ (see Sec. VII A). The equilibrium is calculated, according to the method set out in Ref. 36, using the following model pressure and lowest-order (i.e., cylindrical) safety-factor profiles:

$$p_2(\hat{r}) = 0.1\,(1 - \hat{r})^3, \tag{346}$$

$$q_0(\hat{r}) = \frac{3.15\,\hat{r}^2}{1 - (1 - \hat{r}^2)^{3.5}}. \tag{347}$$

Figure 1 shows the $p_2(\hat{r})$ profile, as well as the final safety-factor profile, $q(\hat{r})$. These two functions are used to calculate all of the aspect-ratio expanded quantities described in Sec. VII.

The $\hat{r}$-θ flux-coordinate system associated with the equilibrium is shown in Fig. 2. It can be seen that the plasma equilibrium is not up-down-symmetric, and also has a fairly realistic shape.

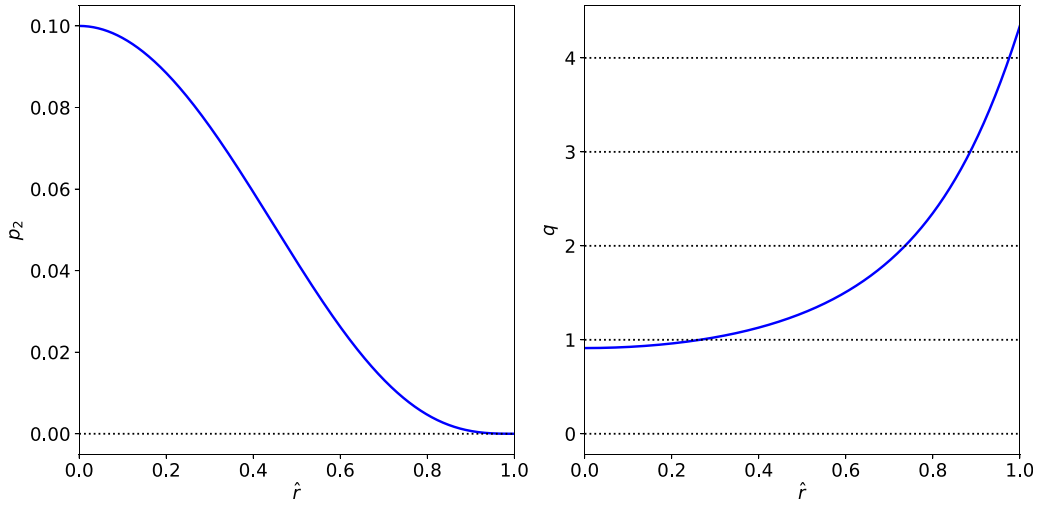

FIG. 1. Normalized pressure and safety-factor profiles for the example tokamak equilibrium.

The locations of the four $n = 1$ rational surfaces in the plasma, as well as the locations of the four toroidal strands that make up the RMP coil system, are shown in Fig. 2.

Finally, the normalized plasma inductance and β values for the example equilibrium are $l_i = 1.55$, $\beta_t = 1.97 \times 10^{-3}$, $\beta_p = 0.415$, and $\beta_N = 0.713$.

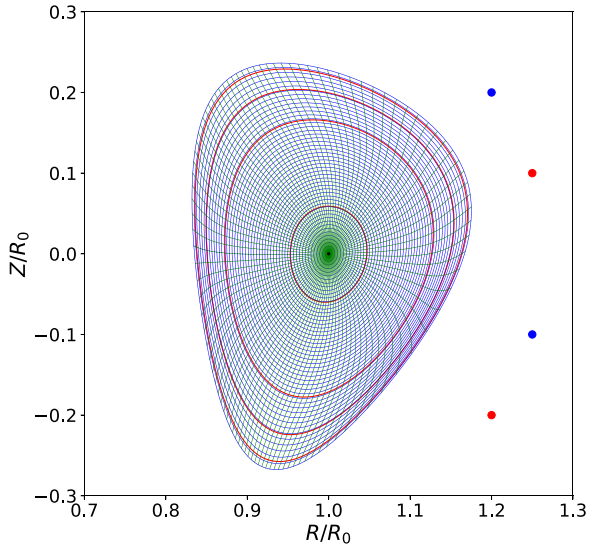

FIG. 2. Flux-coordinate system calculated for the example tokamak equilibrium. Surfaces of constant $\hat{r}$ are shown as blue curves, whereas surfaces of constant θ are shown as green curves. The red curves show the positions of the four $n = 1$ rational magnetic flux surfaces in the plasma. The black dot shows the location of the magnetic axis. The red and blue dots show the positions of the four toroidal strands that make up the RMP coil system. Blue indicates that the toroidal current flowing in the strand is positive, whereas red indicates that it is negative. The magnitudes of the currents are equal.

C. Vacuum response matrix

As described in Sec. VI, the conservation of toroidal electromagnetic angular momentum requires the vacuum response matrix, $H_{m_j m_{j'}} \equiv H_{jj'}$, defined in Eq. (216), to be Hermitian. Here, the m_j, for $j = 0, J$ are the poloidal harmonics included in the calculation. In the present case, $J = 40$, and the m_j range from -15 to $+25$. (Hence, in accordance with the T3/T7 nomenclature, this particular instance of the TJ code could be referred to as the T41 code.) It should be noted that this number of included poloidal harmonics is found to be more than sufficient to obtain converged results for the example equilibrium under investigation.

Consider

$$A_{jj'} = \sum_{j''=0,J} \mathcal{P}^*_{j''j}\, \mathcal{R}_{j''j'}, \tag{348}$$

where $\mathcal{P}_{jj'} \equiv \mathcal{P}^{m_{j'}}_{m_j}$ and $\mathcal{R}_{jj'} \equiv \mathcal{R}^{m_{j'}}_{m_j}$ are defined in Sec. VI D. It is clear from Eq. (216), as well as some standard matrix analysis, that if $H_{jj'}$ is Hermitian then $A_{jj'}$ must also be Hermitian. Figure 3 shows the elements of the $A_{jj'}$ matrix, as well as its anti-Hermitian component,

$$\tilde{A}_{jj'} = \frac{1}{2}\left(A_{jj'} - A^*_{j'j}\right), \tag{349}$$

calculated for the example equilibrium. It can be seen that the elements of $\tilde{A}_{jj'}$ are all considerably smaller than those of $A_{jj'}$, indicating that $A_{jj'}$ is Hermitian to a very good approximation. Let

$$\hat{A}_{jj'} = \frac{1}{2}\left(A_{jj'} + A^*_{j'j}\right) \tag{350}$$

be the Hermitian component of $A_{jj'}$. We can ensure that $H_{jj'}$ is exactly Hermitian by solving

$$\sum_{j''=0,J} \mathcal{P}^*_{j''j}\, \hat{\mathcal{R}}_{j''j'} = \hat{A}_{jj'}, \tag{351}$$

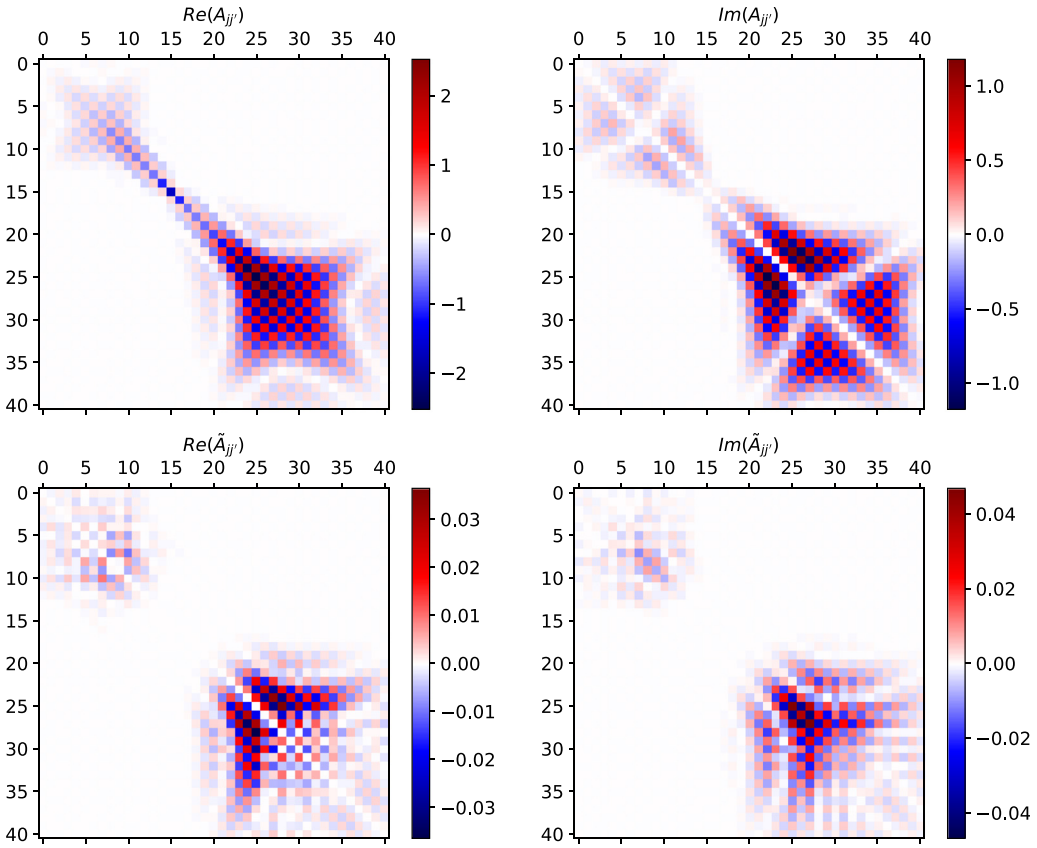

FIG. 3. Elements of the $n = 1$ vacuum matrix $A_{jj'}$, as well as its anti-Hermitian component, $\tilde{A}_{jj'}$, calculated for the example tokamak equilibrium specified in the previous two figures.

$$\sum_{j'=0,J} \hat{\mathcal{R}}^{*}_{j'j} H_{j''j'} = \mathcal{P}^{*}_{j'j} \tag{352}$$

to obtain first $\hat{R}_{jj'}$ and then $H_{jj'}$. Here, use has been made of Eq. (216). The elements of the resulting, exactly Hermitian, vacuum response matrix, $H_{jj'}$, are shown in Fig. 4.

D. Solution of outer-region O.D.E.s

As described in Sec. VII F, the tearing mode eigenfunctions are constructed by launching a set of $J + 1$ linearly independent, well-behaved solutions of the outer-region o.d.e.s from the magnetic axis, and then integrating them to the plasma boundary. At each rational

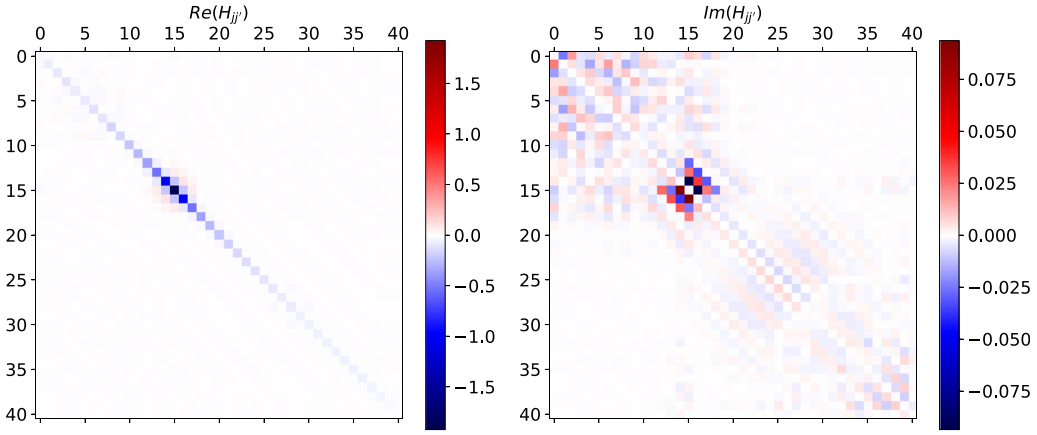

FIG. 4. Elements of the $n = 1$ vacuum response matrix, $H_{jj'}$, calculated for the example tokamak equilibrium specified in Figs. 1 and 2.

surface in the plasma, the solutions satisfy jump conditions that ensure that the coefficients of the large and the small solutions are continuous across the surface. Now, each one of these solutions must conserve the toroidal electromagnetic angular momentum flux, $T_\phi(r)$, that is defined in Eq. (117). This follows because $T_\phi(r)$ is exactly conserved by the outer-region o.d.e.s (102) and (103), provided that the coupling coefficients appearing in these equations satisfy the symmetry constraints (110)–(113) (which they do—see Sec. VII E). Moreover, this conservation property holds irrespective of how many poloidal harmonics are included in the calculation. The jump conditions ensure continuity of $T_\phi(\hat{r})$ across the rational surfaces. However, the launch conditions at the magnetic axis imply that $T_\phi(0) = 0$ (see Sec. VII F). Thus, we conclude that every independent solution of the outer-region o.d.e.s, launched from the magnetic axis, and integrated to the plasma boundary, should be characterized by $T_\phi(\hat{r}) = 0$ throughout the plasma. Obviously, this is a very stringent and powerful test that the integration of the outer-region o.d.e.s is accurate, and also that the jump conditions imposed at the rational surfaces have been correctly formulated.

Figure 5 shows a well-behaved solution of the outer-region o.d.e.s, launched from the magnetic axis, and integrated to the plasma boundary. This particular solution is dominated by the $m = 1$ harmonic close to the axis. It can be seen that $T_\phi(\hat{r})$ is constant between rational surfaces. This demonstrates that the Cash-Karp embedded RK4/RK5 adaptive-step integration scheme press used to solve the outer-region o.d.e.s does so in an accurate manner.[42] It can also be seen that there are small jumps in $T_\phi(\hat{r})$ across the rational surfaces. This occurs because the jump conditions specified in Sec. V are based on an expansion in δ (the closest distance that the outer-region solution approaches the rational surface) and are, therefore, only approximate. However, the spurious jumps in $T_\phi(\hat{r})$ across the rational surfaces are relatively insignificant (a jump of unity would be significant). Moreover, these jumps can be made arbitrarily small by decreasing δ (in the present case $\delta = 10^{-9}$) because the accuracy of the expansion becomes greater as δ decreases. Of course, decreasing δ causes the adaptive integration routine to spend more time in the vicinity of the rational surfaces (recall that the outer-region o.d.e.s are singular at the rational surfaces), so a compromise has to be made. Under normal circumstances, the choice $10^{-8} \leq \delta \leq 10^{-9}$ ensures accurate conservation of angular momentum without unduly slowing down the calculation. (Note that the major results of the code exhibit no dependence on δ when it is this small.)

The construction of the tearing mode eigenfunctions also requires a set of small solutions of the outer-region o.d.e.s, launched from each rational surface in the plasma, and integrated to the plasma boundary (see Sec. VIII C). The launch conditions ensure that the flux of toroidal angular momentum from the rational surface is zero. At each subsequent rational surface in the plasma that the solutions are integrated over, the solutions satisfy jump conditions that ensure that the coefficients of the large and the small solutions are continuous across the

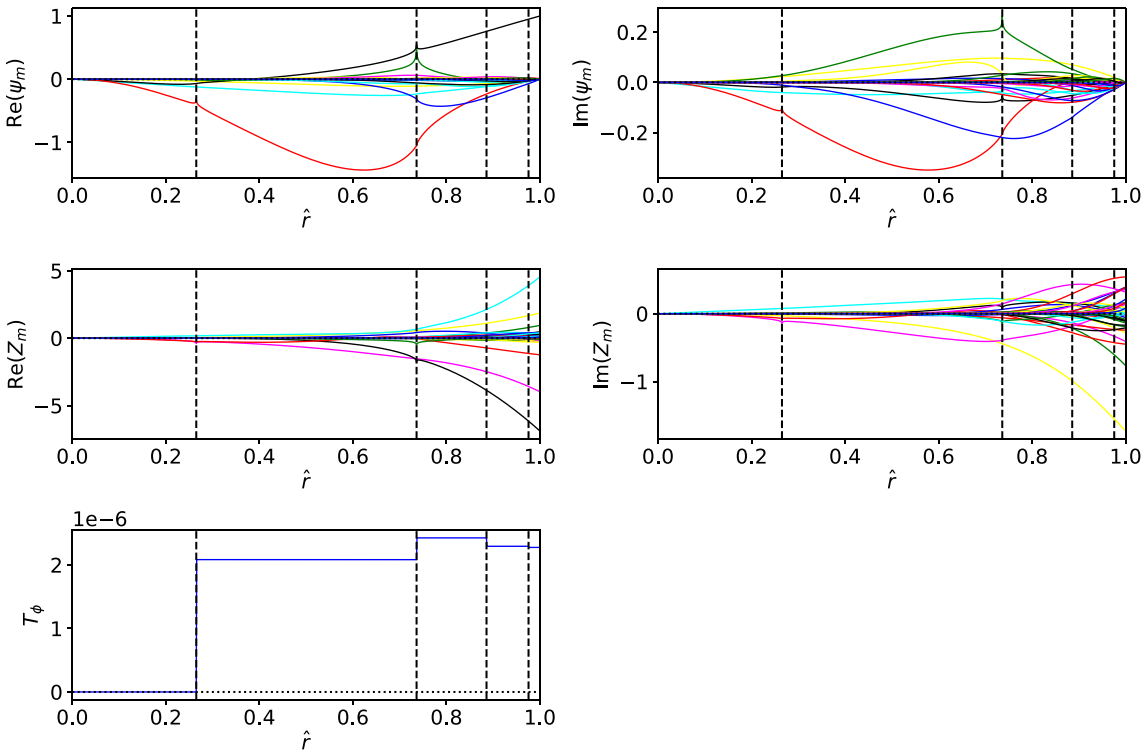

FIG. 5. Poloidal harmonics of a solution of the $n = 1$ outer-region o.d.e.s, launched from the magnetic axis in such a manner that it is dominated by the $m = 1$ harmonic close to the axis. Black curves correspond to $m = 1$, red to $m = 0$ or $m = 2$, green to $m = -1$ or $m = 3$, blue to $m = -2$ or $m = 4$, yellow to $m = -3$ or $m = 5$, cyan to $m = -4$ or $m = 6$, magenta to $m = -5$ or $m = 7$, black to $m = -6$ or $m = 8$, etc. The vertical dashed lines show the locations of the $n = 1$ rational surfaces. Here, $T_\phi(\hat{r})$ is the toroidal electromagnetic angular momentum flux associated with the solution.

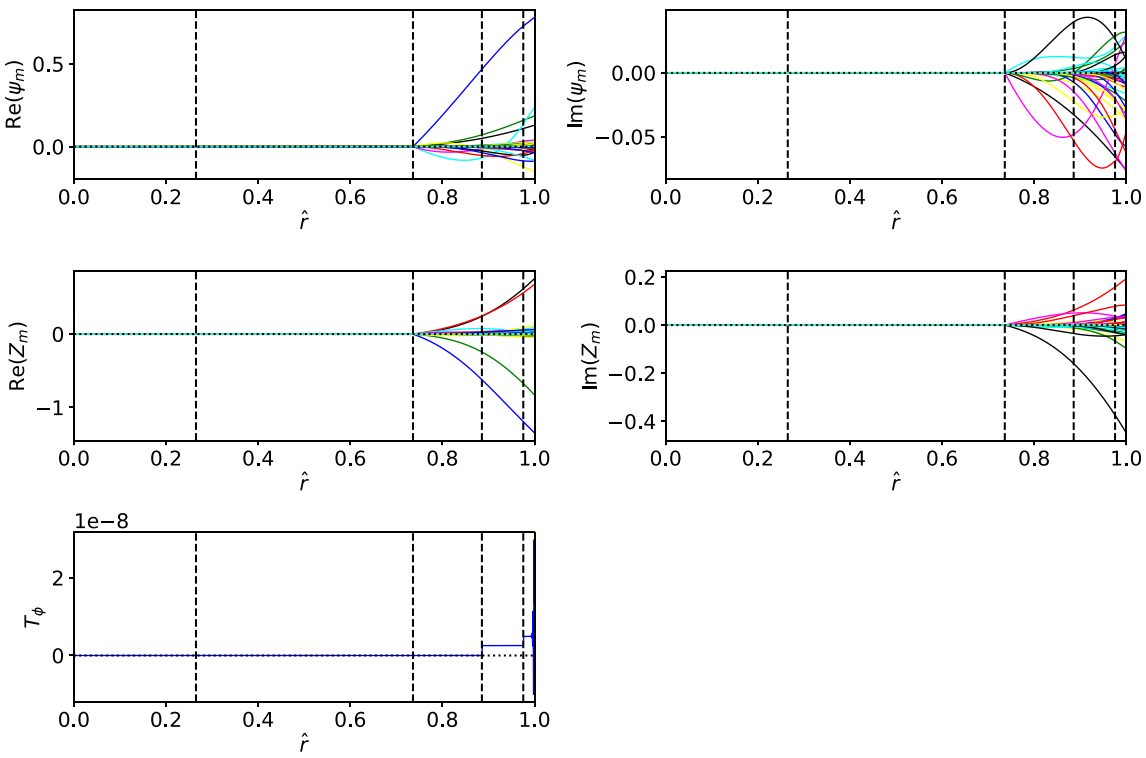

FIG. 6. Poloidal harmonics of a "small" solution of the $n = 1$ outer-region o.d.e.s, launched from the $q = 2$ surface. Black curves correspond to $m = 2$, red to $m = 1$ or $m = 3$, green to $m = 0$ or $m = 4$, blue to $m = -1$ or $m = 5$, yellow to $m = -2$ or $m = 6$, cyan to $m = -3$ or $m = 7$, magenta to $m = -4$ or $m = 8$, black to $m = -5$ or $m = 9$, etc. The vertical dashed lines show the locations of the $n = 1$ rational surfaces. Here, $T_\phi(\hat{r})$ is the toroidal electromagnetic angular momentum flux associated with the solution.

surface. Thus, by analogy with the previous discussion, each small solution launched from a rational surface should be characterized by $T_\phi(\hat{r}) = 0$ throughout the plasma. Again, this is a very stringent test of both the integration algorithm and the jump conditions.

Figure 6 shows a small solution launched from the $q = 2$ surface. It can be seen that $T_\phi(\hat{r})$ is very small throughout the plasma, indicating that integration algorithm and jump conditions are working properly.

E. Tearing eigenfunctions

As described in Sec. VIII D, an unreconnected tearing eigenfunction is constructed from a linear combination of the well-behaved solutions of the outer-region o.d.e.s launched from the magnetic axis, and small solutions launched from the rational surfaces. The mix of the various solutions that make up the combination is influenced by the vacuum response matrix. There is an independent unreconnected tearing eigenfunction for each rational surface in the plasma.

Figures 7 and 8 show the unreconnected tearing eigenfunctions associated with the $q = 1$ and the $q = 2$ rational surfaces. Both of these solutions should be associated with zero toroidal electromagnetic angular momentum flux throughout the plasma. It can be seen that this is the case, to a very good approximation. Figure 9 shows the toroidal electromagnetic angular momentum flux, $T_\phi(\hat{r})$, associated with a general complex linear combination of the unreconnected eigenfunctions pictured in Figs. 7 and 8. This figure exhibits three key features:

1. $T_\phi(\hat{r})$ is constant between rational surfaces: this must be the case because the outer-region o.d.e.s exactly conserve T_ϕ.
2. $T_\phi(\hat{r})$ is zero inside the innermost rational surface: this must be the case otherwise a net electromagnetic torque would be exerted at the magnetic axis, which is unphysical.
3. $T_\phi(\hat{r})$ is zero outside the outermost rational surface: this must be the case otherwise there would be a flux of toroidal electromagnetic angular momentum across the plasma boundary, implying that the plasma exerts a net toroidal electromagnetic torque on itself, which is unphysical.

The fact that $T_\phi(\hat{r})$ is non-zero and constant between the $q = 1$ and $q = 2$ surfaces implies that these surfaces (or, to be more exact, the non-ideal plasmas in the inner regions centered on these surfaces) exert equal and opposite toroidal electromagnetic torques on one another. Note that the toroidal angular momentum flux calculated from every possible pair of tearing eigenfunctions must satisfy the previous three criteria. This constitutes an important self-consistency check on the calculation. Incidentally, the T3 and T7 codes fail this test badly, except at very small values of the inverse aspect ratio (i.e., $\epsilon \lessapprox 0.01$).

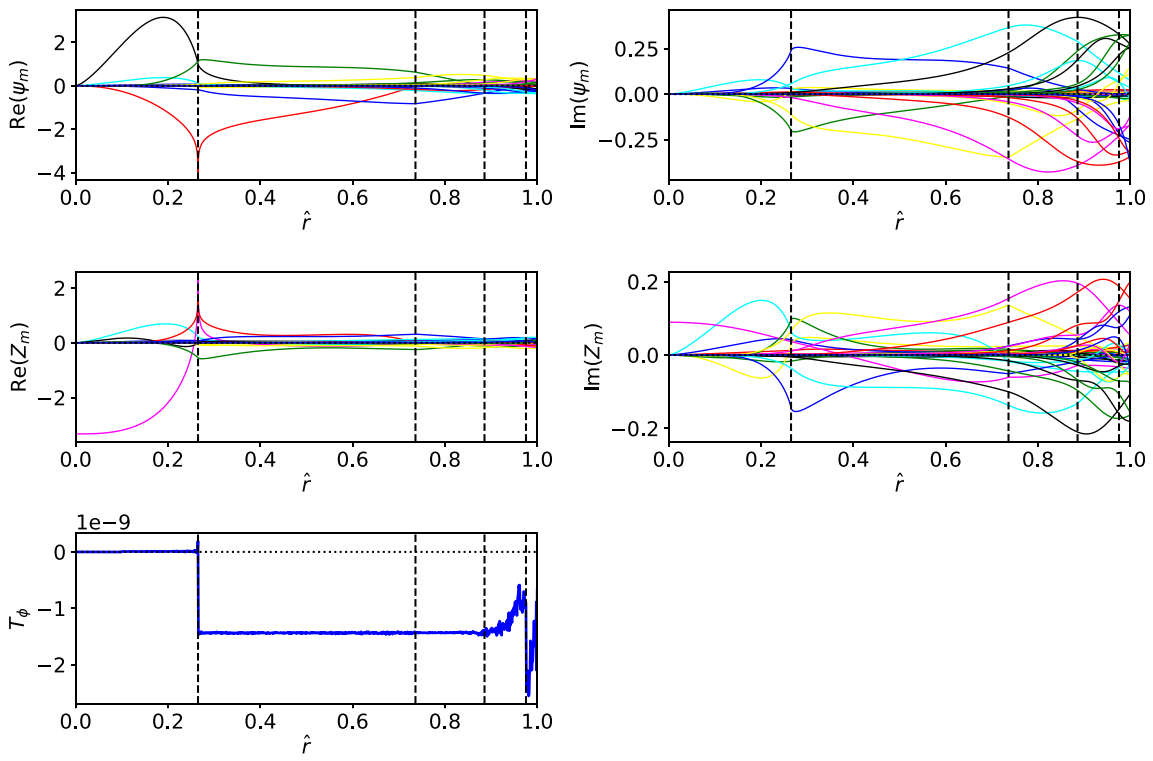

FIG. 7. Poloidal harmonics of the "unreconnected" $n = 1$ tearing eigenfunction associated with the $q = 1$ surface. Black curves correspond to $m = 1$, red to $m = 0$ or $m = 2$, green to $m = -1$ or $m = 3$, blue to $m = -2$ or $m = 4$, yellow to $m = -3$ or $m = 5$, cyan to $m = -4$ or $m = 6$, magenta to $m = -5$ or $m = 7$, black to $m = -6$ or $m = 8$, etc. The vertical dashed lines show the locations of the $n = 1$ rational surfaces. Here, $T_\phi(\hat{r})$ is the toroidal electromagnetic angular momentum flux associated with the eigenfunction.

F. Toroidal tearing mode stability matrix

As described in Sec. VIII D, the general homogeneous toroidal tearing mode dispersion relation can be written as

$$\sum_{k'=1,4} (\Delta_k \, \delta_{kk'} - E_{kk'}) \, \Psi_{k'} = 0. \tag{353}$$

for $k = 1, 4$. Here, k indexes the four $n = 1$ rational surfaces in the plasma: namely, the $m = 1/n = 1$, $m = 2/n = 1$, $m = 3/n = 1$, and $m = 4/n = 1$ surfaces. Moreover, Δ_k is the complex inner-region layer response index at the kth rational surface,[6] whereas Ψ_k is the reconnected helical magnetic flux at the surface. Finally, $E_{kk'}$ is the toroidal tearing mode stability matrix.[3,6] As discussed in Sec. VIII E, the $E_{kk'}$ matrix must be Hermitian; otherwise, an isolated tokamak plasma would be able to exert a net toroidal electromagnetic torque on itself, which is unphysical.

Table I shows the toroidal tearing mode matrix calculated for the example equilibrium. It can be seen that the matrix is Hermitian to a very high degree of accuracy. This constitutes yet another important internal check on the accuracy of the calculation.

Now, the Δ_k indices are functions of the angular phase velocity, ω, of the tearing mode.[6,28] Tokamak plasmas generally contain sufficient levels of sheared plasma rotation to ensure that if ω is chosen in such a manner as to make $\Delta_k \sim \mathcal{O}(1)$ at the kth rational surface then $|\Delta_{k' \neq k}| \gg 1$ at the other rational surfaces.[6,38] Under these circumstances, the dispersion relation (353) yields

$$\frac{\Psi_{k'}}{\Psi_k} \simeq \frac{E_{k'k}}{\Delta_{k'}} \ll 1, \tag{354}$$

for $k' \neq k$, and

$$\Delta_k \simeq E_{kk}. \tag{355}$$

In other words, we obtain a tearing mode that only reconnects significant amounts of magnetic flux at the kth rational surface, and satisfies the quasi-cylindrical dispersion relation (355).[1] This dispersion relation ensures that ω is determined by the plasma flow at the kth rational surface.[6] It follows that the real quantity E_{kk} can be interpreted as the effective "tearing stability index" for a mode that only reconnects magnetic flux at the kth rational surface. To be more exact, E_{kk} is a measure of the amount of free energy available in the outer region, due to current gradients and pressure gradients,[43] to drive magnetic reconnection at the kth rational surface.

In accordance with the previous discussion, the fact that $E_{11} > 0$, $E_{22} > 0$, $E_{33} < 0$, and $E_{44} < 0$ in Table I suggests that the plasma is subject to four essentially uncoupled $n = 1$ tearing modes. There is an intrinsically unstable (i.e., possessing positive free-energy from the outer region) $m = 1/n = 1$ mode that only reconnects magnetic flux

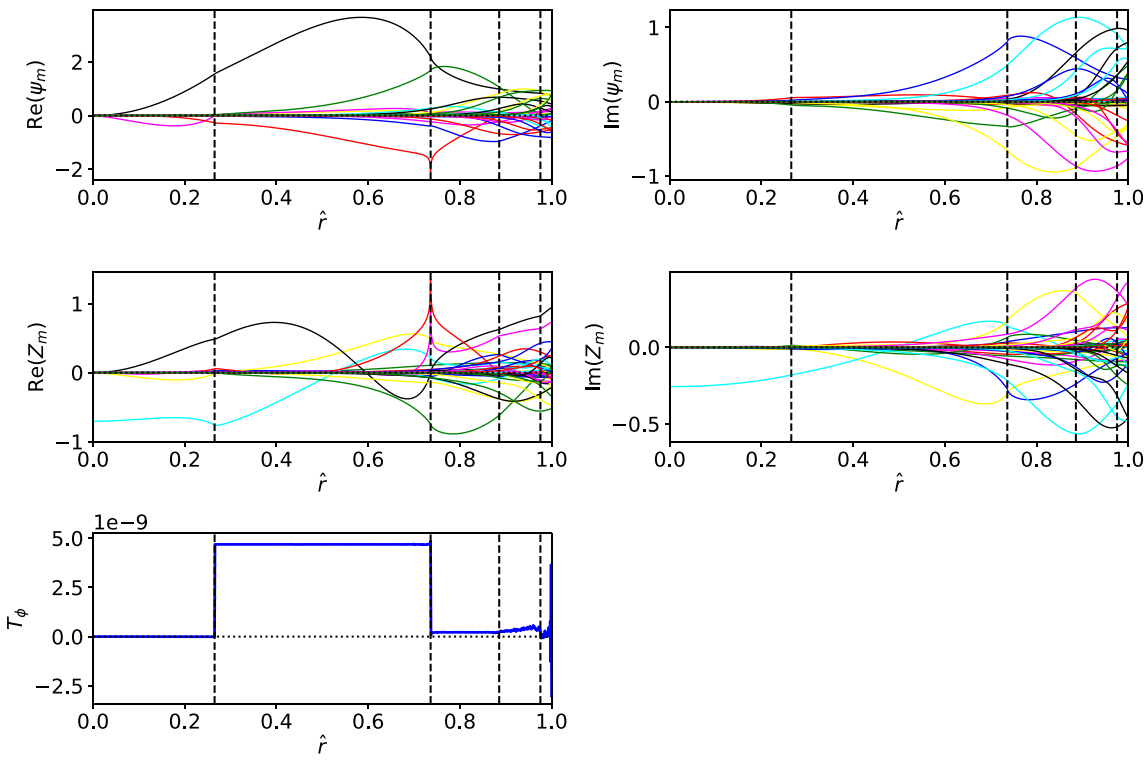

FIG. 8. Poloidal harmonics of the "unreconnected" $n = 1$ tearing eigenfunction associated with the $q = 2$ surface. Black curves correspond to $m = 2$, red to $m = 1$ or $m = 3$, green to $m = 0$ or $m = 4$, blue to $m = -1$ or $m = 5$, yellow to $m = -2$ or $m = 6$, cyan to $m = -3$ or $m = 7$, magenta to $m = -4$ or $m = 8$, black to $m = -5$ or $m = 9$, etc. The vertical dashed lines show the locations of the $n = 1$ rational surfaces. Here, $T_\phi(\hat{r})$ is the toroidal electromagnetic angular momentum flux associated with the eigenfunction.

at the $q = 1$ surface,[1] an intrinsically unstable $m = 2/n = 1$ mode that only reconnects magnetic flux at the $q = 2$ surface, as well as intrinsically stable $m = 3/n = 1$ and $m = 4/n = 1$ modes. It is interesting to note that the inevitable presence of sheared plasma rotation in tokamak plasmas allows the $n = 1$ tearing stability of a general equilibrium to be described by a small number of real stability indices, namely, the diagonal elements of the $E_{kk'}$ matrix.[6] In fact, there are only as many indices as there are $n = 1$ rational surfaces in the plasma. Of course, this constitutes a tremendous simplification over the general case.

Although assuming a "fixed" boundary, which would be the case were the plasma immediately surrounded by a perfectly conducting

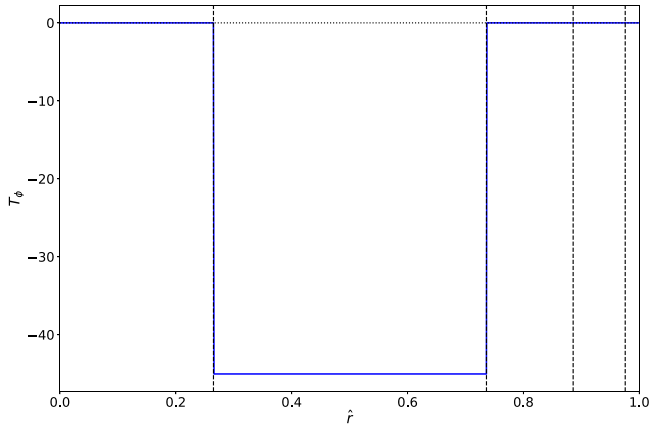

FIG. 9. Toroidal electromagnetic angular momentum flux associated with the tearing eigenfunction pictured in Fig. 7 added to i times the eigenfunction pictured in Fig. 8. The vertical dashed lines show the locations of the $n = 1$ rational surfaces.

TABLE I. Free boundary $n = 1$ toroidal tearing mode stability matrix for the example tokamak equilibrium specified in Figs. 1 and 2.

$\mathrm{Re}(E_{kk'})$:			
$+1.334 \times 10^{1}$	-2.282×10^{0}	$+8.248 \times 10^{-1}$	-3.997×10^{-1}
-2.282×10^{0}	$+3.731 \times 10^{0}$	-2.195×10^{0}	$+2.821 \times 10^{0}$
$+8.247 \times 10^{-1}$	-2.195×10^{0}	-4.319×10^{0}	-2.370×10^{0}
-3.996×10^{-1}	$+2.821 \times 10^{0}$	-2.370×10^{0}	-1.286×10^{1}
$\mathrm{Im}(E_{kk'})$:			
-1.442×10^{-6}	$+4.470 \times 10^{-2}$	$+3.801 \times 10^{-2}$	-9.714×10^{-2}
-4.470×10^{-2}	$+4.900 \times 10^{-8}$	$+9.925 \times 10^{-2}$	$+2.826 \times 10^{-1}$
-3.801×10^{-2}	-9.925×10^{-2}	-1.607×10^{-8}	$+2.811 \times 10^{-1}$
$+9.713 \times 10^{-2}$	-2.826×10^{-1}	-2.811×10^{-1}	-1.146×10^{-8}

TABLE II. Fixed boundary $n = 1$ toroidal tearing mode stability matrix for the example tokamak equilibrium specified in Figs. 1 and 2.

$\mathrm{Re}(E_{kk'})$:			
$+1.312 \times 10^{1}$	-1.784×10^{0}	$+4.305 \times 10^{-1}$	-1.194×10^{-1}
-1.784×10^{0}	$+1.165 \times 10^{0}$	-1.043×10^{0}	$+1.161 \times 10^{0}$
$+4.305 \times 10^{-1}$	-1.043×10^{0}	-1.212×10^{1}	-9.685×10^{-1}
-1.194×10^{-1}	$+1.161 \times 10^{0}$	-9.685×10^{-1}	-5.383×10^{1}
$\mathrm{Im}(E_{kk'})$:			
-8.534×10^{-7}	-1.716×10^{-1}	$+2.297 \times 10^{-1}$	-1.339×10^{-1}
$+1.716 \times 10^{-1}$	$+1.567 \times 10^{-7}$	$+1.292 \times 10^{-1}$	$+1.206 \times 10^{-2}$
-2.297×10^{-1}	-1.292×10^{-1}	$+1.211 \times 10^{-7}$	$+6.702 \times 10^{-1}$
$+1.339 \times 10^{-1}$	-1.206×10^{-2}	-6.702×10^{-1}	-2.545×10^{-7}

wall (which mandates that $\psi = 0$ at $\hat{r} = 1$), is not particularly realistic, we have calculated the fixed-boundary tearing stability matrix of the example equilibrium for the sake of comparison (see Table II). It can be seen that the diagonal elements of the stability matrix are all more negative than the corresponding values shown in Table I, as a consequence of the stabilizing effect of the wall. As expected, the effect is much more marked for modes whose rational surfaces lie closer to the plasma boundary.

G. Response to RMP

As described in Sec. IX E, if the plasma is subject to an $n = 1$ RMP generated by non-axisymmetric currents flowing in external magnetic field coils then, in the presence of sheared plasma rotation, the reconnected magnetic flux driven by the RMP at the kth $n = 1$ rational surface is given by

$$\Psi_k \simeq \frac{\chi_k}{\Delta_k}, \tag{356}$$

whereas the toroidal electromagnetic locking torque exerted by the RMP at the surface is written

$$\delta T_k \simeq 2\pi^2\, n\, \frac{\mathrm{Im}(\Delta_k)}{|\Delta_k|^2}\, |\chi_k|^2. \tag{357}$$

Now, in general, χ_k is proportional to the current, $I_{\rm rmp}$, circulating around the RMP coils. Thus, we can write

$$\chi_k = I_{\rm rmp}\, \hat{\chi}_k, \tag{358}$$

where $\hat{\chi}_k$ is calculated on the assumption that unit current circulates around the RMP coils.

Table III shows the $|\hat{\chi}_k|$ parameters calculated for the example plasma equilibrium and $n = 1$ RMP coil set pictured in Figs. 1 and 2.

TABLE III. RMP drive parameters at the $n = 1$ rational surfaces for the example tokamak equilibrium and $n = 1$ RMP coil set specified in Figs. 1 and 2.

$\lvert\hat{\chi}_k\rvert$:			
9.008×10^{-3}	1.294×10^{-2}	1.262×10^{-2}	1.176×10^{-2}

It is interesting to note that, despite the complexity of the RMP (which requires a great number of poloidal harmonics to fully describe it), and despite the complexity of the plasma response to the RMP (which is a linear combination of 45 independent solutions of the outer-region o.d.e.s, each possessing 41 poloidal harmonics), the ability of the $n = 1$ RMP to either drive magnetic reconnection or to exert electromagnetic locking torques at the four $n = 1$ rational surfaces in the plasma is encapsulated by just four complex numbers, $\hat{\chi}_k$. Again, this constitutes a tremendous simplification.

XI. SUMMARY

In Secs. II–IX, the tearing mode stability of an inverse aspect-ratio expanded tokamak plasma equilibrium with magnetic flux surfaces of general shape is investigated using asymptotic matching techniques. The crucial role played by the conservation of toroidal electromagnetic angular momentum is emphasized throughout the investigation. Note that the inverse aspect-ratio expansion is only introduced in Sec. VII. So, all of the analysis prior to this section is completely general.

The TJ code, which is a specific implementation of the analysis of Secs. II–IX, is described in Sec. X. This code, which is freely available at https://github.com/rfitzp/TJ, represents a significant improvement on the previous T3[4] and T7[6] inverse aspect-ratio expanded toroidal tearing mode codes, because it is constructed in such a manner as to strictly conserve toroidal electromagnetic angular momentum. In fact, as described in Sec. X, the requirement of angular momentum conservation leads to a large number of stringent self-consistency checks that the TJ code must pass in order for its results to be credible. Fortunately, the TJ code passes all of these checks for the example calculation presented in this paper. Unlike the T3 and T7 codes, the TJ code can deal with equilibrium magnetic flux surfaces of arbitrary shape, and, in particular, is not restricted to up-down-symmetric plasma equilibria. Furthermore, unlike the much more general PEST-III,[7] RDCON,[19] and STRIDE[18] toroidal tearing mode codes, the TJ code is comparatively lightweight (there are only about 7000 lines of code) and can easily be run on a laptop computer. Thus, the TJ code is ideal for optimization studies.

In future work, we intend to benchmark the TJ code against the RDCON code. We also intend to add a layer physics module to the code. The layer module will be based on the reduced-MHD analysis of Ref. 44 and will allow us to calculate tearing mode growth-rates, as well as the locking torques generated at the various rational surfaces in the plasma by an RMP. It turns out that the information generated by the TJ code can, in principle, be used to calculate the ideal-MHD δW matrix.[25] Hence, we intend to add an ideal stability module to the code (because there is little point in studying the resistive stability of an ideally unstable plasma). Other envisaged improvements to the code include the addition of a resistive wall, as well as the calculation of neoclassical viscous torques.

ACKNOWLEDGMENTS

This research was directly funded by the U.S. Department of Energy, Office of Science, Office of Fusion Energy Sciences, under Contract No. DE-SC0021156. The analytic calculations described this paper have been verified using the REDUCE computer algebra system, which is available at https://reduce-algebra.sourceforge.io. The TJ code is freely available at https://github.com/rfitzp/TJ.

AUTHOR DECLARATIONS

Conflict of Interest

The author has no conflicts to disclose.

Author Contributions

Richard Fitzpatrick: Conceptualization (equal); Formal analysis (equal); Investigation (equal); Methodology (equal); Writing – original draft (equal).

DATA AVAILABILITY

The data that support the findings of this study are available from the corresponding author upon reasonable request.

APPENDIX: NONORTHOGONAL CURVILINEAR COORDINATES

Consider the nonorthogonal curvilinear coordinate system, r, θ, and ϕ, introduced in Sec. II A, and let $\mathcal{J} = (\nabla r \times \nabla\theta \cdot \nabla\phi)^{-1}$.

Let

$$\mathbf{A} = A^r\, \mathcal{J}\, \nabla\theta \times \nabla\phi + A^\theta\, \mathcal{J}\, \nabla\phi \times \nabla r + A^\phi\, \mathcal{J}\, \nabla r \times \nabla\theta, \quad \text{(A1)}$$

$$\mathbf{A} = A_r\, \nabla r + A_\theta\, \nabla\theta + A_\phi\, \nabla\phi, \quad \text{(A2)}$$

where $\mathbf{A}$ is a general vector. It is easily demonstrated that

$$\mathbf{A}\cdot\mathbf{B} = A_r\, B^r + A_\theta\, B^\theta + A_\phi\, B^\phi = A^r\, B_r + A^\theta\, B_\theta + A^\phi\, B_\phi, \quad \text{(A3)}$$

$$(\mathbf{A}\times\mathbf{B})_r = \mathcal{J}\,(A^\theta\, B^\phi - A^\phi\, B^\theta), \quad \text{(A4)}$$

$$(\mathbf{A}\times\mathbf{B})_\theta = \mathcal{J}\,(A^\phi\, B^r - A^r\, B^\phi), \quad \text{(A5)}$$

$$(\mathbf{A}\times\mathbf{B})_\phi = \mathcal{J}\,(A^r\, B^\theta - A^\theta\, B^r), \quad \text{(A6)}$$

$$\mathcal{J}\,(\mathbf{A}\times\mathbf{B})^r = A_\theta\, B_\phi - A_\phi\, B_\theta, \quad \text{(A7)}$$

$$\mathcal{J}\,(\mathbf{A}\times\mathbf{B})^\theta = A_\phi\, B_r - A_r\, B_\phi, \quad \text{(A8)}$$

$$\mathcal{J}\,(\mathbf{A}\times\mathbf{B})^\phi = A_r\, B_\theta - A_\theta\, B_r, \quad \text{(A9)}$$

where $\mathbf{B}$ is another general vector. Furthermore,

$$\mathcal{J}\,\nabla\cdot\mathbf{C} = \frac{\partial(\mathcal{J}\,C^r)}{\partial r} + \frac{\partial(\mathcal{J}\,C^\theta)}{\partial\theta} + \frac{\partial(\mathcal{J}\,C^\phi)}{\partial\phi}, \quad \text{(A10)}$$

$$\mathcal{J}\,(\nabla\times\mathbf{C})^r = \frac{\partial C_\phi}{\partial\theta} - \frac{\partial C_\theta}{\partial\phi}, \quad \text{(A11)}$$

$$\mathcal{J}\,(\nabla\times\mathbf{C})^\theta = \frac{\partial C_r}{\partial\phi} - \frac{\partial C_\phi}{\partial r}, \quad \text{(A12)}$$

$$\mathcal{J}\,(\nabla\times\mathbf{C})^\phi = \frac{\partial C_\theta}{\partial r} - \frac{\partial C_r}{\partial\theta}, \quad \text{(A13)}$$

where $\mathbf{C}(\mathbf{r})$ is a general vector field.

REFERENCES

[1]H. P. Furth, J. Killeen, and M. N. Rosenbluth, Phys. Fluids **6**, 459 (1963).
[2]J. W. Connor and R. J. Hastie, "The effect of shaped plasma cross sections on the ideal kink mode in a tokamak," Technical Report CLM-M106 (Culham Laboratory, Abingdon UK, 1985).
[3]J. W. Connor, R. J. Hastie, and J. B. Taylor, Phys. Fluids B **3**, 1539 (1991).
[4]J. W. Connor, S. C. Cowley, R. J. Hastie, T. C. Hender, A. Hood, and T. J. Martin, Phys. Fluids **31**, 577 (1988).
[5]A. Pletzer and R. L. Dewar, J. Plasma Phys. **45**, 427 (1991).
[6]R. Fitzpatrick, R. J. Hastie, T. J. Martin, and C. M. Roach, Nucl. Fusion **33**, 1533 (1993).
[7]A. Pletzer, A. Bondeson, and R. L. Dewar, J. Comput. Phys. **115**, 530 (1994).
[8]Y. Nishimura, J. D. Callen, and C. C. Hegna, Phys. Plasmas **5**, 4292 (1998).
[9]S. A. Galkin, A. D. Turnbull, J. M. Greene, and M. S. Chu, Phys. Plasmas **7**, 4070 (2000).
[10]S. Tokuda, Nucl. Fusion **41**, 1037 (2001).
[11]D. P. Brennan, R. J. La Haye, A. D. Turnbull, M. S. Chu, T. H. Jensen, L. L. Lao, T. C. Luce, P. A. Politzer, E. J. Strait *et al.*, Phys. Plasmas **10**, 1643 (2003).
[12]C. J. Ham, Y. Q. Liu, J. W. Connor, S. C. Cowley, R. J. Hastie, T. C. Hender, and T. J. Martin, Plasma Phys. Controlled Fusion **54**, 105014 (2012).
[13]C. J. Ham, J. W. Connor, S. C. Cowley, C. G. Gimblett, R. J. Hastie, T. C. Hender, and T. J. Martin, Plasma Phys. Controlled Fusion **54**, 025009 (2012).
[14]C. J. Ham, J. W. Connor, S. C. Cowley, R. J. Hastie, T. C. Hender, and Y. Q. Liu, Plasma Phys. Controlled Fusion **55**, 125015 (2013).
[15]A. H. Glasser, Z. R. Wang, and J.-K. Park, Phys. Plasmas **23**, 112506 (2016).
[16]R. Fitzpatrick, Phys. Plasmas **24**, 072506 (2017).
[17]A. S. Glasser, E. Kolemen, and A. H. Glasser, Phys. Plasmas **25**, 032507 (2018).
[18]A. S. Glasser and E. Koleman, Phys. Plasmas **25**, 082502 (2018).
[19]Z. Wang, A. H. Glasser, D. Brennan, Y. Liu, and J.-K. Park, Phys. Plasmas **27**, 122503 (2020).
[20]J. M. Greene, J. L. Johnson, and K. E. Weimer, Phys. Fluids **14**, 671 (1971).
[21]R. Fitzpatrick, C. G. Gimblett, and R. J. Hastie, Plasma Phys. Controlled Fusion **34**, 161 (1992).
[22]M. S. Chance, Phys. Plasmas **4**, 2161 (1997).
[23]T. Xu and R. Fitzpatrick, Nucl. Fusion **59**, 064002 (2019).
[24]M. N. Bussac, R. Pellat, D. Edery, and J. L. Soule, Phys. Rev. Lett. **35**, 1638 (1975).
[25]J. P. Freidberg, *Ideal Magnetohydrodynamics* (Plenum, New York, 1987).
[26]R. Iacono, A. Bondeson, F. Troyon, and R. Gruber, Phys. Fluids B **2**, 1794 (1990).
[27]L. Guazzotto, R. Betti, J. Manickam, and S. Kaye, Phys. Plasmas **11**, 604 (2004).
[28]R. Fitzpatrick, Nucl. Fusion **33**, 1049 (1993).
[29]A. H. Glasser, J. M. Greene, and J. L. Johnson, Phys. Fluids **18**, 875 (1975).
[30]C. Mercier, Nucl. Fusion **1**, 47 (1960).
[31]R. Fitzpatrick, Phys. Plasmas **1**, 3308 (1994).
[32]P. M. Morse and H. Feshbach, *Methods of Theoretical Physics* (McGraw-Hill, New York, 1953), p. 1301.
[33]P. M. Morse and H. Feshbach, *Methods of Theoretical Physics* (McGraw-Hill, New York, 1953), p. 1302.
[34]M. Abramowitz and I. A. Stegun, *Handbook of Mathematical Functions* (Dover, New York, 1964), Sec. 8.11.
[35]M. Abramowitz and I. A. Stegun, *Handbook of Mathematical Functions* (Dover, New York, 1964), Chap. 6.
[36]R. Fitzpatrick, Phys. Plasmas **31**, 082505 (2024).
[37]V. D. Shafranov, Sov. At. Energy **13**, 1149 (1963).
[38]R. Fitzpatrick, *Tearing Mode Dynamics in Tokamak Plasmas* (IOP, Bristol, UK, 2023).
[39]R. Fitzpatrick, Phys. Plasmas **5**, 3325 (1998).
[40]A. Cole and R. Fitzpatrick, Phys. Plasmas **13**, 032503 (2006).
[41]R. Fitzpatrick and A. O. Nelson, Phys. Plasmas **27**, 072501 (2020).
[42]W. H. Press, S. A. Teukolsky, W. T. Vetterling, and B. P. Flannery, *Numerical Recipes in C*, 2nd ed. (Cambridge University Press, Cambridge, UK, 1992), Sec. 16.2.
[43]I. B. Bernstein, E. A. Frieman, M. D. Kruskal, and R. M. Kulsrud, Proc. R. Soc. London Ser. A **244**, 17 (1958).
[44]R. Fitzpatrick, Phys. Plasmas **29**, 032507 (2022).